



**HAL**  
open science

## Detecting ecological signatures of long-term human activity across an elevational gradient in the Šumava Mountains, Central Europe

Vachel Kraklow, Dagmar Dreslerová, Andrei-Cosmin Diaconu, Alice Moravcová, Martin Kadlec, Daniel Nývlt, Willy Tinner, Marco Heurich, Walter Finsinger, Angelica Feurdean, et al.

### ► To cite this version:

Vachel Kraklow, Dagmar Dreslerová, Andrei-Cosmin Diaconu, Alice Moravcová, Martin Kadlec, et al.. Detecting ecological signatures of long-term human activity across an elevational gradient in the Šumava Mountains, Central Europe. *Quaternary Science Reviews*, 2024, 344, pp.108944. 10.1016/j.quascirev.2024.108944 . hal-04700848

**HAL Id: hal-04700848**

**<https://hal.science/hal-04700848v1>**

Submitted on 21 Nov 2024

**HAL** is a multi-disciplinary open access archive for the deposit and dissemination of scientific research documents, whether they are published or not. The documents may come from teaching and research institutions in France or abroad, or from public or private research centers.

L'archive ouverte pluridisciplinaire **HAL**, est destinée au dépôt et à la diffusion de documents scientifiques de niveau recherche, publiés ou non, émanant des établissements d'enseignement et de recherche français ou étrangers, des laboratoires publics ou privés.

**This is a copy of the ‘submitted version’ of the paper:**

**Kraklow VA, Dreslerová D, Diaconu A-C, Moravcová A, Kadlec M, Nývlt D, Tinner W, Heurich M, Finsinger W, Feurdean A, *et al.* 2024.** Detecting ecological signatures of long-term human activity across an elevational gradient in the Šumava Mountains, Central Europe. *Quaternary Science Reviews* **344**: 108944.

Please refer to the published version that is available online (<https://dx.doi.org/10.1016/j.quascirev.2024.108944>) or contact any of the Authors for a complimentary copy.

1 Detecting ecological signatures of long-term human activity across an elevational gradient in the  
2 Šumava Mountains, Central Europe

3

4 Vachel A. Carter<sup>\*1,2,3</sup>, Dagmar Dreslerová<sup>4</sup>, Andrei-Cosmin Diaconu<sup>5</sup>, Alice Moravcová<sup>1</sup>, Martin  
5 Kadlec<sup>6</sup>, Daniel Nývlt<sup>6</sup>, Willy Tinner<sup>7</sup>, Marco Heurich<sup>8,9,10</sup>, Walter Finsinger<sup>11</sup>, Angelica  
6 Feurdean<sup>12</sup>, Petr Kuneš<sup>1</sup>, Gabriela Florescu<sup>1,13</sup>

7

8 <sup>1</sup> Department of Botany, Charles University, Prague, Czechia

9 <sup>2</sup> Department of Geography, University of Utah, Salt Lake City, Utah, USA

10 <sup>3</sup> Earth and Environmental Sciences Division, Los Alamos National Laboratory, Los Alamos,  
11 NM, USA

12 <sup>4</sup> Institute of Archaeology of the Czech Academy of Sciences, Praha, Czechia

13 <sup>5</sup> Department of Geology, Babeş-Bolyai University, Kogalniceanu, 1, 400084, Cluj-Napoca,  
14 Romania

15 <sup>6</sup> Department of Geography, Masaryk University, Brno, Czech Republic

16 <sup>7</sup> Institute of Plant Sciences and Oeschger Centre for Climate Change Research, University of  
17 Bern, Switzerland

18 <sup>8</sup> Department of National Park Monitoring and Animal Management, Bavarian Forest National  
19 Park, Freyunger Str. 2, 94481 Grafenau, Germany

20 <sup>9</sup> Chair of Wildlife Ecology and Management, Faculty of Environment and Natural Resources,  
21 University of Freiburg, Tennenbacher Straße 4, 79106 Freiburg, Germany

22 <sup>10</sup> Institute of Forestry and Wildlife Management, Inland Norway University of Applied Science,  
23 NO-2480 Koppang, Norway

24 <sup>11</sup> ISEM, University of Montpellier, CNRS, IRD, Montpellier, France

25 <sup>12</sup> Department of Physical Geography, Goethe University, Altenhöferallee 1, 60438 Frankfurt am  
26 Main, Germany

27 <sup>13</sup> Department of Geography, Stefan cel Mare University of Suceava, Romania

28

29 \*Corresponding author: [vachel.carter@gmail.com](mailto:vachel.carter@gmail.com)

30

31 Written for: Quaternary Science Reviews

32

33 Keyword: peat bog, testate amoebae, water table depth, hydroclimate, fire, pollen, plant  
34 macrofossils, climate change, human impact, Holocene, generalized additive models

35

36

37

38

39

40

41  
42  
43  
44  
45  
46  
47  
48  
49  
50  
51  
52  
53  
54  
55  
56  
57  
58  
59  
60  
61

## **Abstract**

Central European mountains, including the Šumava Mountains located along the Czechia/Germany border, have a long and rich anthropogenic history. Yet, documenting prehistoric human impact in central European mountain environments remains a challenge because of the need to disentangle climate and human-caused responses in terrestrial systems. Here, we present the first reconstructed water table depths (WTDs) from two sites, Pěkná and Blatenská slat', located in the Šumava Mountains. We compare these local hydroclimate records with new and published pollen, non-pollen palynomorphs (NPPs), plant macrofossils, geochemistry and archeological records to investigate how hydroclimate and human activities impacted forest succession and fire activity throughout the Holocene across an elevational gradient. Using a generalized additive model, our results suggest that changes in forest succession and fire activity have been primarily caused by climate throughout the Holocene. However, humans have been utilizing mountain environments and their resources continuously since ~4600–4250 cal yr BP, thus playing a secondary role in modifying forest succession to increase resources beneficial to both humans and grazers. Over the last 1000 years, we provide evidence of directly observed human-caused modifications to the landscape. These results contribute to a growing body of literature illustrating human activities and landscape modifications in central European mountains.

## **1. Introduction**

European mountain environments have a long and rich history with humans, particularly the Alps and Carpathians (Schmidl et al., 2005; Lutz and Pernicka, 2013; Geantă et al., 2014; Kothieringer et al., 2015; Feurdean et al., 2016; Schumacher et al., 2016; Finsinger et al., 2018; Gilck and Poschlod, 2019; Carter et al., 2020; Florescu et al., 2024). For example, alpine farming in the Alps has been a beneficial style of land use after 7000–6500 cal yr BP, with the most unambiguous evidence starting ~4200 cal yr BP, due to the vast open grasslands which were utilized by humans and livestock during the summer season (Hafner and Schwörer, 2018; Gilck and Poschlod, 2019; Tinner, 2023; Tinner et al., 2023). In the Carpathians, mountain farming has been documented since ~4400–3500 cal yr BP across a wide spectrum of elevations (Geantă et al., 2014; Feurdean et al., 2016; Feurdean et al., 2017; Lestienne et al., 2023). However, despite having a rich archeological history in the lowlands, it is believed that human impact in Central European mountains with lower elevations was less intense than in other European mountains (Rösch, 2000; Robin et al., 2013; Henkner et al., 2018) likely because of local contingencies, including the occurrence of denser forests and the lack of a treeless alpine zone (Dreslerová et al., 2020a). Documenting prehistoric human impact in Central European mountains remains a challenge, which inhibits our ability to assess potential legacies of past environmental changes, including past land uses, on contemporary forest structure and function (Willis and Birks, 2006), which ultimately also influence modern forest succession (Josefsson et al., 2009).

81  
82 One of Central Europe's largest forested landscapes is located along the Czechia-Germany  
83 border (Šumava National Park, Czechia, and Bavarian Forest National Park, Germany).  
84 Together, both National Parks form the great Bohemian Forest Ecosystem and are part of the  
85 Natura 2000 network and UNESCO Biosphere Reserve, which was established to protect the  
86 most endangered flora and fauna in Central Europe (Krzystek et al., 2020). Upper Palaeolithic  
87 and Mesolithic archeological sites have been found at high elevations in the Šumava Mountains  
88 (Dreslerová et al., 2020b), with pollen taxa indicative of human activity documented since the  
89 Neolithic (Svobodová et al., 2001; Svobodová et al., 2002; Carter et al., 2018a) illustrating that  
90 the region has a long archeological history, making it an ideal place to investigate the extent of  
91 human impact on the landscape (Kozáková et al., 2020). However, there appears to be a  
92 boundary of ~600 m asl separating sub-montane settlements from non-settled land which is  
93 associated with suitable agropastoral farming (Dreslerová et al., 2020a).

94  
95 Previous paleoecological studies from the region have investigated long-term anthropogenic  
96 impacts in the Šumava Mountains (Carter et al., 2018a; Kozáková et al., 2020). Using a  
97 macrophysical climate model to reconstruct local climate, Carter et al. (2018a) suggest increased  
98 fire activity in the early Holocene was likely driven by climate, despite archeological evidence  
99 illustrating high populations of Mesolithic communities in the region. Additionally, Carter et al.,  
100 (2018a) suggest that increased fire activity ~2500 cal yr BP was not climatically-driven, but  
101 instead a result of increased anthropogenic activities which agrees with recent research by  
102 Kozáková et al. (2020) who found increasing anthropogenic impact, including fire activity, since  
103 the Late Bronze and Iron Ages. Both studies suggest that changes in forest succession since the  
104 last millennia were likely due to increasing human activities. However, validating anthropogenic  
105 impacts from paleoecological records from the Šumava Mountains has been challenging because  
106 of the lack of local proxy-based records of climate which are needed to disentangle climate vs  
107 anthropogenically-induced changes. The only local record of climate that exists from the Šumava  
108 Mountains spans the Late Glacial-Early Holocene transition (Mateo-Beneito et al. 2024). While  
109 the macrophysical climate model attempted to separate any anthropogenic signature from  
110 climatically-driven events (Carter et al., 2018a), until now, no local record of Holocene climate  
111 exists from the Šumava Mountains making it difficult to validate that changes in forest  
112 succession and fire activity are driven by human activity, and not from climate.

113  
114 To fill in this gap, we present the first records of hydroclimate associated with long-term climate  
115 changes. Specifically, we present reconstructed water table depths (WTDs) from two new peat  
116 bog records, one from a mid-elevation locality located near the 600 m asl agropastoral boundary  
117 (Pěkná, 730 m asl), and one from a high elevation locality (Blatenská slat', 1275 m asl) to  
118 investigate whether the ecological impact of human activities varied spatially across an elevation  
119 gradient. Ombrotrophic peat bogs are excellent recorders of past hydrological changes due to  
120 their surface being directly coupled to rainfall, temperature, and humidity (Blackford, 2000). As

121 such, these depositional environments may be useful in disentangling climate versus  
122 anthropogenically-induced changes in vegetation assemblages and fire regimes. By comparing a  
123 local record of climate (via testate amoebae reconstructed WTDs) with new and published  
124 pollen, non-pollen palynomorphs (NPPs), plant macrofossils, geochemistry (see Schafstall et al.,  
125 2024) and archeological records, we aim to determine how 1) Holocene hydroclimate patterns  
126 varied across an elevational gradient and how changes in hydroclimate impacted forest  
127 succession and fire activity throughout the Holocene, and 2) whether changes in forest  
128 succession and fire activity were caused by climate and/or humans.

129

## 130 **2. Study Sites**

131 Pěkná (48°50'26.451", 13°56'14.9922") is a mid-elevation (730 m asl) peat bog located in an  
132 open valley near the village of Pěkná on the southern margin of the Šumava National Park  
133 (Figure 1). Pěkná is comprised of three bogs that span an area of 1.38 km<sup>2</sup>, with the coring  
134 locality being located in the middle bog; the middle bog's area is 0.7 km<sup>2</sup>. The peat bog is ~50 m  
135 from the Vltava River and ~5 km from Lipno reservoir. Pěkná is located <12 km from known  
136 Mesolithic and Bronze Age archeological sites and is roughly ~15 km from the nearest historic  
137 trading route (Dreslerová et al., 2020b). Local vegetation consists of mostly bog pine (*Pinus*  
138 *rotundata*), with *Betula pubescens*, *Pinus sylvestris*, and *Picea abies* towards the bog edge. Herb  
139 and shrub vegetation consists of *Sphagnum* sp., *Vaccinium* sp., *Eriophorum vaginatum*,  
140 *Andromeda polifolia*, *Oxycoccus palustris*, and *Melampyrum*.

141

142 By contrast, Blatenská slat' (48°58'19.227"N, 13°27'18.699"E) is a high elevation (1275 m asl)  
143 raised peat bog located at the highest point in the Modravské slatě bog complex saddled between  
144 Blatný vrch peak and Studená hora peak near the village of Modrava (Schafstall et al., 2024)  
145 (Figure 1). The bog, with a size of 0.71 km<sup>2</sup>, includes two large and several smaller peatland  
146 ponds. Blatenská slat' is located <10 km from known Mesolithic archeological sites and is  
147 roughly ~10 km from the nearest historic trading route. Blatenská slat' is approximately 33 km  
148 from the Pěkná peat bog. Local vegetation is covered by hummocks and hollows comprised of  
149 *Andromeda polifoliae-Sphagnetum magellanici* with marginal zones formed by *Pinus uncinata*  
150 subsp. *uliginosa* (Neuman) Businsky and shrub layers of *Vaccinium myrtillus*. Towards the bog  
151 edge and regionally, *Picea abies* dominates with a stand of *Abies alba* ~2 km away (Schafstall et  
152 al., 2024).

153

## 154 **3. Methods**

### 155 **3.1 Core retrieval**

156 In June 2019, sediment cores were extracted from Pěkná, and in October 2019, sediment cores  
157 were extracted from Blatenská slat'. For Pěkná, a 419 cm composite sediment profile composed  
158 of two cores (PEK1 and PEK2) was extracted from the center of the Pěkná peat bog (48.8420614  
159 N, 13.9382436 E). PEK 1 was extracted using a prototype percussion corer with a sediment  
160 chamber of 3 m in length and 10 cm in diameter, and PEK 2 with a modified Livingstone piston

161 corer with a sediment chamber of 1 m in length and a diameter of 6 cm (Merkt and Streif, 1970).  
162 The upper-most 254 cm of continuous, undisturbed peat was collected from the first core  
163 (PEK1), and the lower portion of the composite profile (165 cm) was collected from PEK2. Core  
164 correlation was done on the overlapping sequence based on visual peat stratigraphy and magnetic  
165 susceptibility data. Peat cores were transported to Charles University where they were  
166 subsampled at 1 cm intervals for paleoecological analysis.

167  
168 For Blatenská slat', two parallel cores (BL1 and BL2) totaling 319 cm in depth were collected  
169 from the center of Blatenská slat' using a modified Livingstone piston corer (see Schafstall et al.,  
170 2024 for further details).

### 171 **3.2 Geochronology and Radiocarbon dating**

173 For Pěkná, peat age-depth relations were established using thirteen  $^{14}\text{C}$  dates of bulk peat and  
174 macrofossils and a  $^{210}\text{Pb}$  series using a Bayesian method in rbacon package in R (Blaauw and  
175 Christen, 2011) (see Table 1). All  $^{14}\text{C}$  dates were calibrated using the IntCal20 dataset (Reimer et  
176 al., 2020) (Figure 2). All measured ages were included using a Student-t distribution for  $^{14}\text{C}$  ages  
177 and a normal distribution for  $^{210}\text{Pb}$  ages. Based on lithology, two sedimentation zones were  
178 implemented in the age-depth model by adding a boundary at 350 cm and constraining their  
179 mean accumulation rate by 20 yr/cm for the upper part and 50 yr/cm for the lower part. The age-  
180 depth model partitioned the core into 85 sections, estimating the accumulation rate for each  
181 segment using a Markov Chain Monte Carlo (MCMC) approach.

182  
183 For Blatenská slat', twelve  $^{14}\text{C}$  dates of bulk peat and macrofossils, and a  $^{210}\text{Pb}$  series were used  
184 to create peat age-depth relations (for details see Schafstall et al., 2024). All  $^{14}\text{C}$  dates from both  
185 sites were analyzed at Isotoptech Zrt. located in Debrecen, Hungary, and the  $^{210}\text{Pb}$  profile was  
186 analyzed at the Faculty of Science, Institute of Geochemistry, Mineralogy and Mineral  
187 Resources, Charles University.

### 188 189 **3.3 Testate Amoebae analysis and water table reconstruction**

190 Testate amoebae were used to reconstruct water table depth (i.e., groundwater levels) at both  
191 sites. Testate amoebae were analyzed at 3–5 cm intervals for both Pěkná and Blatenská slat'  
192 using 1 cm<sup>3</sup> of sediment per sample. The samples were prepared following standard procedures  
193 (Hendon and Charman, 1997). At least 150 testate amoebae shells were counted and identified at  
194 each level under a stereomicroscope at 400× magnification using available taxonomic  
195 classifications (e.g. Mazei and Tsyganov, 2006). The quantitative reconstruction of water table  
196 depth was obtained using the pan-European transfer function of Amesbury et al. (2016).

### 197 198 **3.4 Analysis of paleoclimate simulations**

199 Following Schafstall et al. (2024), we retrieved simulated climatic variables (mean annual  
200 temperature (MAT °C), temperature of the wettest quarter of the year (T WetQ (°C)), and

201 precipitation of the wettest quarter of the year (WetQ PP (mm)) for the past 12,500 years from  
202 the CHELSA climate database (Karger et al., 2023). All data were first cropped to a 1 km  
203 window around Pěkná and Blatenská slat', and then the resulting values were extracted from .tif  
204 files using R statistical software (R Core Team, 2023).

205

### 206 **3.5 Geochemical analysis and magnetic susceptibility**

207 Geochemistry and magnetic susceptibility were used to investigate erosional and depositional  
208 activity at both sites. Elemental composition was determined using X-ray fluorescence  
209 spectroscopy (XRF). Individual dried (at 37 °C) samples in plastic bags were analyzed with a  
210 hand-held Innov-X DELTA analyzer in Geochem-Vanad mode. The total measurement time (6  
211 minutes) was automatically divided into two phases: heavy elements (beam 40 kV) and light  
212 elements (beam 10 kV). Similarly, magnetic susceptibility was measured on the same samples.  
213 Using the Kappabridge MFK1-FA (AGICO, Inc.), which allows directly measuring mass-  
214 specific magnetic susceptibility ( $\chi$ ), the samples were analyzed at two frequencies (low 976 Hz  
215 and high 15,616 Hz) with an induced magnetic field of 200 A·m<sup>-1</sup>. Low-frequency magnetic  
216 susceptibility ( $\chi_{LF}$ ) and high-frequency magnetic susceptibility ( $\chi_{HF}$ ) were then obtained, but we  
217 only present  $\chi_{LF}$ . We then verified through experimentation that plastic bags do not affect the  
218 mentioned analyses. In both cases, the values are many orders of magnitude lower, as they are  
219 made of diamagnetic material and thus do not significantly skew the results.

220

221 For both sites, heavy metal and carbonate-related elements (i.e., Fe, Ca, Pb) were normalized  
222 with Zr, which is the most stable lithogenic element within our record, to differentiate the source  
223 of Fe and Ca since these elements can have both authigenic and allogenic origin (Engstrom and  
224 Wright, 1984; Boyle, 2001). We also used the ratio, Rb/Sr, as an indicator of weathering  
225 intensity in each catchment (Chen et al., 1999).

226

### 227 **3.6 Pollen, coprophilous fungi, plant macrofossils, and pollen richness and diversity**

228 Pollen analysis was used to reconstruct regional changes in vegetation at Pěkná and Blatenská  
229 slat'. Pollen analysis was conducted contiguously at 2 cm resolution from both sites (see  
230 Schafstall et al., 2024). Pollen processing utilized acid-base rinse procedures following Faegri et  
231 al. (1989) using 1 cm<sup>3</sup> of sediment per sample. For both Pěkná and Blatenská slat', two  
232 *Lycopodium* tablets (X=9,666 grains/tablet, Batch #3862) were added to each sample prior to  
233 pollen processing and used as an exotic tracer to calculate both pollen concentration (grains cm<sup>3</sup>)  
234 and pollen accumulation rates (pollen influx; grains cm<sup>-2</sup> yr<sup>-1</sup>) (Stockmarr, 1972). A minimum of  
235 500 terrestrial pollen grains were identified at a magnification of 400× with the aid of  
236 identification keys (Beug, 2004; Punt, 1976–1996). Pollen counts were converted into pollen  
237 percentages based on the abundance of each pollen type relative to the sum of all identified  
238 terrestrial pollen. To investigate anthropogenic influences at Pěkná and Blatenská slat', we used  
239 anthropogenic pollen indicators (Behre, 1981, 1988; Behre et al., 2023) which were grouped  
240 following Deza-Araujo et al., 2020: (i) primary anthropogenic indicators (cultivars), (ii)



241 adventive anthropogenic indicators (plants introduced with agriculture), and (iii) apophytes  
242 (native plant species favored by human activities) (Table 2). We also used the ratio of arboreal  
243 (AP) to non-arboreal pollen (NAP) to investigate canopy openness. A ratio of pioneer species  
244 (*Pinus* + *Betula*) to late-successional species (*Picea abies* + *Abies* + *Fagus*) was also used to  
245 investigate trends in forest succession over time. Additionally, coprophilous fungi spores  
246 (*Podospora*, *Sordaria*, *Tripterospora*, and *Sporormiella*) were used to identify grazing by  
247 domestic or wild herbivores (Baker et al., 2013).

248

249 Plant macrofossil analysis was used to explore changes in local vegetation assemblages. For both  
250 sites, plant macrofossils were analyzed using a stereomicroscope at a magnification of 15–50×  
251 and were identified with the aid of identification keys (Cappers et al., 2006; Bojňanský and  
252 Fargašová, 2007; Katz et al., 1977; Tomlinson, 1985) and the herbarium collection at Charles  
253 University. For Pěkná, macrofossils analysis was conducted every 2–3 cm and concentrations of  
254 plant macrofossils were adjusted to a constant volume of 15 cm<sup>3</sup> using procedures described by  
255 Birks (2007). For Blatenská slat', macrofossil analysis was conducted every 2 cm on average,  
256 with the top 14 cm pooled into one sample due to low sample size (see Schafstall et al., 2024).  
257 Plant macrofossils were not adjusted to a constant volume, and instead were presented as  
258 percentages, not concentrations.

259

260 To investigate biodiversity dynamics at each site, we calculated pollen-assemblage richness and  
261 diversity (Hill, 1973) following Finsinger et al. (2017). Specifically, we calculated N0, which is  
262 the total number of taxa in an assemblage, N1 which is the number of common taxa, and N2  
263 which is the number of dominant taxa (Hill, 1973). Instead of using an analytical approach  
264 (Birks and Line, 1992), we resampled randomly and without replacement the pollen counts 1000  
265 times to the smallest sample size (here n = 177 for Pěkná, and 514 for Blatenská slat') prior to  
266 estimating N0, N1, and N2, to provide mean estimates and 95% confidence intervals of N0, N1,  
267 and N2 (Felde et al., 2016). Evenness was estimated as the ratio of dominant taxa relative to all  
268 taxa present in an assemblage using the N2/N0 ratio (Birks et al., 2016a). Pollen-assemblage  
269 richness and diversity were calculated following Finsinger et al., (2017) using the 'vegan'  
270 package (Oksanen et al., 2016) in R (R Core Team, 2023).

271

### 272 **3.7 Charcoal analysis**

273 Microscopic-charcoal was counted simultaneously with pollen analysis on the pollen slides  
274 (Finsinger and Tinner, 2005) at a magnification of 400× and was used to reconstruct regional fire  
275 activity (Tinner et al., 1998). Microscopic charcoal counts were transformed to concentrations  
276 (particles cm<sup>-3</sup>) and charcoal accumulation rates (CHAR; the number of particles cm<sup>-2</sup> yr<sup>-1</sup>)  
277 using the software program, Tilia (Grimm, 2004). Macroscopic charcoal was used to reconstruct  
278 local-to-regional fire activity at Pěkná and Blatenská slat'. Macroscopic charcoal was analyzed at  
279 1 cm resolution at Pěkná and 0.5 cm resolution at Blatenská slat' using sub-samples of 2 cm<sup>3</sup>  
280 from each site. Samples from both sites were left in 10 ml of sodium hexametaphosphate for 24

281 hr to disaggregate organic matter, and then 5 ml of sodium hypochlorite (10% NaOCl) to bleach  
282 non-charred material. Macroscopic charcoal was gently sieved through a 125  $\mu\text{m}$  sieve and was  
283 analyzed using a stereomicroscope at a magnification of 15–50 $\times$ .

284  
285 Macrocharcoal morphologies were used to reconstruct the type of biomass burned from each site  
286 (i.e., a qualitative metric of fuel burnt/fire intensity) (Umbanhowar and Mcgrath, 1998; Enache  
287 and Cumming, 2006). Macrocharcoal morphologies were identified following Enache and  
288 Cumming (2006) and Mustaphi and Pisaric (2014), and were classified as wood, herb, grass and  
289 undifferentiated. Macroscopic charcoal counts, including macrocharcoal morphologies, were  
290 transformed to concentrations (particles  $\text{cm}^{-3}$ ) and charcoal accumulation rates (CHAR; the  
291 number of particles  $\text{cm}^{-2} \text{yr}^{-1}$ ). Macroscopic charcoal counts were then broken into a low-  
292 frequency component, known as charcoal background (BCHAR), and a peaks component  
293 (CHARpeak) using an interpolated temporal resolution of 30-years  $\text{sample}^{-1}$  (for Pěkná) and 35-  
294 years  $\text{sample}^{-1}$  (for Blatenská slat') using the program, CharAnalysis (Higuera et al., 2009).  
295 BCHAR was determined using a robust LOWESS regression with a moving-window width of  
296 900 years (for Pěkná) and 1000 years (for Blatenská slat') which resulted in a robust signal-to-  
297 noise index (SNI)  $> 3.0$  (Kelly et al., 2011). CHARpeak values were calculated as residuals from  
298 BCHAR and were separated from the background noise with a locally defined threshold using  
299 the 99th percentile of a Gaussian mixture model. The identified CHARpeaks were then screened  
300 with a minimum count peak-screening test (Higuera et al., 2010).

301

### 302 **3.8 Statistical Analyses**

303 To disentangle climate versus human-induced activities across an elevational gradient, we used a  
304 multivariate generalized additive model (GAM; Hastie and Tibshirani, 1986) implemented in the  
305 'mgcv' package (Wood, 2006). To account for the high temporal variability within each of the  
306 time-series, all datasets were first binned into 100-year intervals by taking the average of each  
307 binned window. We then tested the relationships between hydroclimate (i.e., WTD) and humans  
308 (i.e., the sum of primary and adventive pollen indicators) set as the predictor variables, and  
309 different response variables that document changes in vegetation, fire and geochemistry.

310 Additionally, because many of the primary and adventive pollen indicators are included in the  
311 NAP sum, we removed these taxa from the NAP sum to ensure these taxa were not biasing the  
312 GAM results. In each simulation, we used a Gaussian distribution with an identity link function.

313

314 A principal component analysis (PCA) was used to describe the main features of the  
315 palynological record and assess whether the primary, adventive and apophyte pollen taxa  
316 clustered together. Correlation matrices were used using PAST software (Hammer et al., 2001).

317

## 318 **4 Results**

### 319 **4.1 Chronology and core lithology**

320 The calibrated modeled mean basal age for Pěkná is 12,600 cal yr BP (Figure 2). Peat deposition  
321 rates were relatively steady with a mean of 30 years per centimeter throughout the entire record.  
322 The lower unit of the Pěkná peat core (12,640-11,430 cal yr BP) contains *Carex* peat with  
323 decomposed fragments of ligneous and herbaceous materials along with fine and coarse sand (SI  
324 Figure 1). Sand disappears from the Pěkná peat core ~11,279 cal yr BP and *Carex* continues to  
325 dominate until ~8850 cal yr BP. A transition to *Eriophorum* peat was recorded at 8850 cal yr BP  
326 until ~7900 cal yr BP. *Sphagnum* peat with *Eriophorum* then dominates until 6500 cal yr BP, and  
327 then switches to *Eriophorum* peat until 2500 cal yr BP. Brief episodes of *Sphagnum*-dominated  
328 peat occurred during that time frame, specifically between 5400–5200 cal yr BP and 4700–3900  
329 cal yr BP. The profile then briefly switches to *Sphagnum* peat ~2500 cal yr BP until 1700 cal yr  
330 BP when it returns to *Eriophorum* peat mixed with Ericaceae roots until ~500 cal yr BP. The last  
331 500 years have been *Sphagnum*-dominated peat (SI Figure 1).

332

333 The calibrated basal age for Blatenská slat' is 7300 cal yr BP (Schafstall et al., 2024). Peat  
334 deposition rates were relatively steady with a mean of 20 years per centimeter throughout the  
335 entire record. The lithology of the Blatenská slat' is mainly comprised of reddish brown or dark  
336 brown slightly fibrous decomposed material, except between 4800–4450 cal yr BP (depths  
337 ~182–210 cm) and the last ~100 years (i.e., the top 10cm), which is comprised of slightly  
338 reddish/dark brown undecomposed peat (see Schafstall et al. 2024). *Sphagnum medium*/*S.*  
339 *divinum* dominates throughout the entire profile, with *S. cf angustifolium* only being present from  
340 7300–2000 cal yr BP (SI Figure 2). *Sphagnum fuscum* and *S. sect. acutifolia* are also only  
341 present between 5500–4500 cal yr BP.

342

#### 343 4.2. Reconstructed water table depth

344 At Pěkná, reconstructed WTDs were low, ranging between 28–20 cm below the peat surface  
345 starting ~10,500 until 7500 cal yr BP, with a period of extremely low values ~28–27 cm between  
346 9750–9200 cal yr BP (Figure 3). *Cryptodiffugia oviformis* and *Cryptodiffugia pusilla* are high  
347 between 12,500–8000 cal yr BP before decreasing; in the case of *C. pusilla* it disappears from  
348 the record entirely (SI Figure 3). Around 8000 cal yr BP, *Archerella flavum* and *Assulina*  
349 *muscorum* increase and dominate along with *D. pulex*. Other taxa that appear ~8000–7500 cal yr  
350 BP include *Arcella catinus*, *Assulina seminulum*, *Bullinularia indica*, *Heleopera petricola*, and  
351 *Hyalosphenia elegans*. WTDs increased starting ~7500 cal yr BP and remained relatively high,  
352 oscillating between 18-10 cm until ~1600 cal yr BP before decreasing again in conjunction with  
353 *Archerella flavum* and *Assulina muscorum* dominance. WTDs remained low between 1600–0 cal  
354 yr BP, ranging between 24–20 cm in conjunction with *Cryptodiffugia oviformis* dominance,  
355 before quickly increasing again over the modern period.

356

357 At Blatenská slat', reconstructed WTDs show similar patterns as Pěkná, with generally higher  
358 values (between 18–8 cm) between 7300–2200 cal yr BP in conjunction with *Archerella flavum*  
359 dominance (SI Figure 4). WTDs decrease ~2200 cal yr BP and remain low, ranging between 26-

360 24 cm until ~400 cal yr BP in conjunction with a rise in *Cryptodiffugia oviformis* and *Nebela*  
361 *militaris* dominance. WTDs slightly increased over the last few centuries to 16 cm.

362

### 363 4.3. Reconstructed minerogenic component changes

364 At Pěkná, minerogenic input (Rb/Sr) was very strong between 12,600–11,000 cal yr BP and  
365 again between 9500–8200 cal yr BP (Figure 3). Minerogenic input has also increased since the  
366 turn of the 20<sup>th</sup> century. Authigenic Ca and Fe (Ca/Zr and Fe/Zr) both increase ~10,500 cal yr BP  
367 (Figure 3). However, the increase in Ca is short-lived while Fe remains high until ~6200 cal yr  
368 BP. Authigenic Ca increases again between 8000–5500 cal yr BP and over the last 500 years.  
369 Pb/Zr has only been present at high values in the last 2000 years.  $\chi_{LF}$  shows several sporadic  
370 erosional events ~7200, 6000 and 3000 cal yr BP, before increasing over the last 1000 years  
371 (Figure 3).

372

373 At Blatenská slat', minerogenic input is generally low until ~4500 cal yr BP, then sporadically  
374 fluctuates until ~2500 cal yr BP before remaining high until present (Figure 3). Authigenic Ca  
375 and Fe are both high at the onset of the record until ~4500 cal yr BP when both decline. Ca  
376 increases again between ~3300–2000 cal yr BP and then between 500–100 cal yr BP. Pb/Zr is  
377 only present, at high values, over the last 1000 years.  $\chi_{LF}$  shows relatively high erosional activity  
378 between 7300–4200 cal yr BP and then a dramatic increase over the last 50 years (Figure 3).

379

### 380 4.4 Reconstructed vegetation history

381 Locally, the Pěkná peat bog was dominated by *Carex* (*C. rostrata*, *C. cf. canescens*, *C. cf. elata*,  
382 *C. sp.*) from 12,600–8000 cal yr BP before transitioning to *Eriophorium vaginatum* (SI Figure 5).  
383 *Eriophorium vaginatum* macrofossils were consistently present throughout the entire record.

384 Regionally, pioneer species, *Pinus* and *Betula* pollen, dominated the forest canopy at Pěkná  
385 between 12,642–7500 cal yr BP, averaging 42% and 13%, respectively. The AP:NAP ratio was  
386 low during the same time frame, but increases and remains high between 8200–1000 cal yr BP  
387 (Figure 4). *Picea abies* pollen percentages begin to increase ~8500 cal yr BP, and rise to  
388 dominance between 8500–3500 cal yr BP, ranging between 20%–73%. Between 3500 and -42  
389 cal yr BP, *Picea abies* pollen percentages increase averaging 19% of the total pollen rain, and  
390 then increase to an average of 30% over the last 70 years. *Corylus* pollen is present at Pěkná, but  
391 at relatively low percentages (average of 13%) between 12,642–6150 cal yr BP. The  
392 Pioneer:Successional ratio begins to decrease ~8500 cal yr BP, switching to a successional-  
393 dominated forest ~7300 cal yr BP. *Corylus* pollen decreases ~6050 cal yr BP, ranging from 1–  
394 9% from 6050 cal yr BP present. *Fagus* pollen begins to increase ~7950 cal yr BP, remaining  
395 <5% of the total pollen rain between 7950–6400 cal yr BP. *Fagus* pollen increases and fluctuates  
396 between 8%–23% between 6400–280 cal yr BP, and then decreases to <5% of the total pollen  
397 rain until the present. *Abies* pollen first appears ~6350 cal yr BP and averages <3% of the total  
398 pollen rain until ~5500 cal yr BP. *Abies* then increases to an average of 18% between 5500–650  
399 cal yr BP before decreasing to <2% at present. *Pinus* undiff. pollen percentages begin to increase

400 ~3500 cal yr BP, averaging 20% until ~1150 cal yr BP, and then increasing dramatically to an  
401 average of 34% in the last millennia (reaching a maximum of 51% at the turn of the 20<sup>th</sup>  
402 century). AP:NAP decreases over the previous 1000 years, overlapping with an increase in  
403 Pioneer:Successional values at Pěkná. Rarefied pollen richness (N0) shows generally low values  
404 throughout the entire record, except for over the last 1000 years (Figure 4). Pollen evenness  
405 (N2/N0) shows elevated diversity between 9000–7500 cal yr BP and again between 4000–1000  
406 cal yr BP. Apophyte percentages have been present since the onset of the record, with high  
407 percentages (>2%) between 12500–11000 cal yr BP and again over the last 1500 years, peaking  
408 at 8% ~74 cal yr BP. Whereas adventive pollen percentages were first documented ~11,150 cal  
409 yr BP, which was one finding of *Polygonum aviculare*-type (SI Figure 5). Adventives, being  
410 comprised primarily of *Plantago lanceolata*, appear consistently starting ~4600 cal yr BP at low  
411 values (<1%) before peaking ~2% at 150 cal yr BP. Primary pollen indicators first appear 1450  
412 cal yr BP with the arrival of *Secale*, and peak ~3% ~260 cal yr BP. Coprophilous fungi were  
413 found at Pěkná but in low percentages (<2%). *Sordaria* was the most common coprophilous  
414 fungi sporadically found; ~8500 and 8000 cal yr BP, between 3500–750 cal yr BP, and over the  
415 last 500 years. *Podospora* was also found but was less common than *Sordaria*; ~4800 cal yr BP,  
416 ~2500 cal yr BP, and in the last 300 years. *Tripterospora* was found at 3750 cal yr BP and again  
417 sporadically between 400–74 cal yr BP.

418  
419 At Blatenská slat', the local peat bog was dominated by *Sphagnum medium/divinum* and  
420 *Eriophorium vaginatum* the entire Holocene, with occasional findings of *S. cf. angustifolium*, *S.*  
421 *sect. Acutifolia*, *S. fuscum*, *S. majus* and *S. sect. Subsecunda* (SI Figure 2). Regionally, *Pinus*  
422 pollen percentages are high (maximum of 68%) at the onset of the Blatenská slat' record, which  
423 overlaps with high Pioneer:Successional values (Figure 4). *Pinus* pollen then dramatically  
424 declines to 30% ~7200 cal yr BP as *Picea abies* pollen continues to rise to dominance, averaging  
425 63% between 7200–4250 cal yr BP. *Fagus* pollen is present but low (<6%) at the onset of the  
426 record until ~6600 cal yr BP, and then increases to an average of 16% until the last 100 years.  
427 *Fagus* pollen then decreases to an average of 7%. *Abies* pollen average <2% between 7300–4600  
428 cal yr BP and then dramatically increases to an average of 27% (maximum of 60%) between  
429 4600–250 cal yr BP. *Abies* pollen percentages average 6% over the last 200 years. High AP:NAP  
430 values occur between 6500–4300 cal yr BP, with a brief increase ~5500 cal yr BP. Low AP:NAP  
431 values occur between 4300–2200 cal yr BP and again over the last 1000 years, while high  
432 AP:NAP values briefly occur between 2200–1000 cal yr BP (Figure 4). Low  
433 Pioneer:Successional values are documented between 6500–1500 cal yr BP, with a short-lived  
434 increase in values centered ~4200 cal yr BP. Pioneer:Successional values then increase and  
435 remain high until present. Rarefied pollen richness (N0) at Blatenská slat' shows generally higher  
436 values ~7300–5000 cal yr BP, 4000–3000 cal yr BP and again over the last 1000 years (Figure  
437 4). Pollen evenness (N2/N0) shows a general increasing trend in diversity over time until ~1000  
438 cal yr BP when pollen evenness declines. Apophyte percentages have been present since the  
439 onset of the record, with peaks >2% between 4000–3000 cal yr BP and over the last 1000 years.

440 Additionally, adventives, which are comprised primarily of *Centaurea cyanus* and *Plantago*  
441 *lanceolata*, have been present since the onset of the record, however, have been consistently  
442 present since ~4250 cal yr BP. Primary pollen indicators first appear ~5550 cal yr BP with one  
443 finding of *Cannabis*. However, primary pollen indicators have been consistently present starting  
444 ~950 cal yr BP. *Sordaria* was sporadically found ~6500 cal yr BP and over the last 1000 years.  
445 *Podospora* was only found ~6500 and ~4200 cal yr BP.

446

#### 447 **4.5 Reconstructed fire history**

448 At Pěkná, local biomass burning (i.e., CHAR) was generally low throughout the record, except  
449 between 8500–7000 cal yr BP, ~6600 cal yr BP and ~5800 cal yr BP when biomass burning  
450 increased (Figure 7). Fire frequency was at its maximum ~10,500 cal yr BP. Fire frequency  
451 ranged from 2–3 fires/1000 years between 8000–3500 cal yr BP before declining to <1 fire/1000  
452 years at present. Charred macrofossils and microCHAR generally follow the same pattern as  
453 CHAR (Figure 7). The analysis of morphology-based fuel types revealed that wood CHAR  
454 dominated with an average of 0.07 particles cm<sup>-2</sup> yr<sup>-1</sup> throughout the record (Figure 7), reaching  
455 a maximum of 2.7 particles cm<sup>-2</sup> yr<sup>-1</sup> at ~5550 cal yr BP. Grass CHAR averaged 0.07 particles  
456 cm<sup>-2</sup> yr<sup>-1</sup> the entire record, reaching a maximum ~8100 cal yr BP. Other noticeable grass CHAR  
457 events occurred ~6300 cal yr BP, ~6250 cal yr BP, and 5550 cal yr BP. Herb CHAR averaged  
458 0.22 particles cm<sup>-2</sup> yr<sup>-1</sup> throughout the record with seven peaks greater than 2 particles cm<sup>-2</sup> yr<sup>-1</sup>;  
459 ~7600, ~8670 cal yr BP, ~8000 cal yr BP, ~7650 cal yr BP, ~7700 cal yr BP, ~7660, and ~8650.

460

461 At Blatenská slat', local biomass burning was low throughout most of the Holocene, except at the  
462 onset of the record ~7250–6500 cal yr BP (Figure 7). Fire frequency was high for this site at the  
463 onset of the record between 7250–5650 cal yr BP and again over the last 250 years. Between  
464 3700–2400 cal yr BP, fire frequency declined to 0 fires/1000 years. Only six fire episodes were  
465 detected from the Blatenská slat' record. Wood CHAR averaged 0.1 particles cm<sup>-2</sup> yr<sup>-1</sup>  
466 throughout the record with a maximum of 0.27 particles cm<sup>-2</sup> yr<sup>-1</sup> at 6500 cal yr BP (Figure 7).  
467 Grass CHAR averaged 0.01 particles cm<sup>-2</sup> yr<sup>-1</sup> throughout the record with a peak at ~6500 cal yr  
468 BP. Finally, Herb CHAR averaged 0.1 particles cm<sup>-2</sup> yr<sup>-1</sup> with a maximum ~7000 cal yr BP. No  
469 charred macrofossils were identified from Blatenská slat' during macrofossil analysis.

470 Regionally, biomass burning also follows a similar pattern as CHAR (Figure 7).

471

#### 472 **4.6 Generalized Additive Models**

##### 473 **4.6.1. Climate response curves**

474 When investigating the response between hydroclimate and forest succession variables, response  
475 curves illustrate a statistically significant decreasing relationship between WTD and the AP:NAP  
476 ratio (p<0.0124), and a significant increasing relationship with the Pioneer:Successional ratio  
477 (p<0.00001) (Figure 5). No significant relationships were found between WTD and pollen  
478 richness (p=0.525), pollen evenness (p=0.338), and coprophilous fungi (p=0.496). WTD was  
479 found to have a significant relationship with sedimentation rate (p<0.0344), the Fe/Zr ratio

480 ( $p < 0.00001$ ), and the Rb/Sr ratio ( $p < 0.00001$ ) (Figure 6). Additionally, no significant relationship  
481 was found between WTD and the Ca/Zr ratio ( $p = 0.0622$ ), although this is trending towards  
482 significant. Finally, when investigating the response between hydroclimate and fire variables,  
483 response curves for Pěkná show a statistically significant increasing relationship with CHAR  
484 ( $p < 0.0145$ ), grass CHAR ( $p < 0.0262$ ), charred macrofossils ( $p < 0.00556$ ), and microcharcoal  
485 ( $p < 0.00001$ ) (Figure 8). In significant relationships were found between WTD and wood CHAR  
486 ( $p = 0.116$ ) and herb CHAR ( $p = 0.38$ ) (not shown in figures).

487  
488 Response curves for Blatenská slat' illustrate significant relationships between hydroclimate and  
489 the Pioneer:Successional ratio ( $p < 0.000271$ ), pollen richness ( $p < 0.0878$ ), and pollen evenness  
490 ( $p < 0.0222$ ) (Figure 5). No significant relationships were found between climate and the AP:NAP  
491 ratio ( $p = 0.988$ ). Significant relationships were found between hydroclimate and the Ca/Zr ratio  
492 ( $p < 0.000134$ ), the Fe/Zr ratio ( $p < 0.00001$ ) and the Rb/Sr ratio ( $p < 0.00001$ ) (Figure 6). No  
493 significant relationship was found between WTD and sedimentation rate ( $p = 0.283$ ) at Blatenská  
494 slat'. Lastly, modeled response curves suggest no significant relationships between hydroclimate  
495 and fire variables; CHAR ( $p = 0.363$ ), grass CHAR ( $p = 0.329$ ), micro-charcoal ( $p = 0.714$ ) (Figure  
496 8). No significant relationships were found between climate and wood CHAR ( $p = 0.759$ ) and  
497 herb CHAR ( $p = 0.374$ ) (not shown).

498

#### 499 **4.6.2. Anthropogenic response curves**

500 For Pěkná, significant relationships were found between primary and adventive pollen indicators  
501 and coprophilous fungi ( $p < 0.00001$ ), and pollen richness ( $p < 0.00001$ ) (Figure 5). Insignificant  
502 relationships were found with the AP:NAP ratio ( $p = 0.196$ ), the Pioneer:Successional ratio  
503 ( $p = 0.194$ ), pollen evenness ( $p = 0.347$ ) (Figure 5), the Ca/Zr ratio ( $p = 0.224$ ), Fe/Zr ratio  
504 ( $p = 0.093$ ), Rb/Sr ratio ( $p = 0.424$ ), and sedimentation rate ( $p = 0.0826$ ) (Figure 6), and CHAR  
505 ( $p = 0.176$ ), grass CHAR ( $p = 0.228$ ), microcharcoal ( $p = 0.892$ ), charred macrofossils ( $p = 0.185$ )  
506 (Figure 8). Additionally, no significant relationship was found between primary and adventive  
507 pollen indicators and wood CHAR ( $p = 0.318$ ) and herb CHAR ( $p = 0.386$ ) (not shown). The only  
508 significant relationships found between apophyte pollen indicators at Pěkná were with  
509 AP:NAP ( $p < 0.00001$ ), pioneer:successional ( $p < 0.0299$ ), pollen evenness ( $p < 0.00161$ ), pollen  
510 richness ( $p < 0.00001$ ), coprophilous fungi ( $p < 0.00001$ ) (SI Figure 6), and sedimentation rate  
511 ( $p = 0.0122$ ) (SI Figure 7). No significant relationships were found with apophytes and Ca/Zr  
512 ( $p = 0.0912$ ), Fe/Zr ( $p = 0.136$ ), and Rb/Sr ( $p = 0.381$ ) (SI Figure 7), or any fire variable; CHAR  
513 ( $p = 0.258$ ), Grass CHAR ( $p = 0.249$ ), charred macrofossils ( $p = 0.23$ ), microCHAR ( $p = 0.398$ ) (SI  
514 Figure 8), herb CHAR ( $p = 0.681$ ), or wood CHAR ( $p = 0.534$ ) (not shown).

515

516 Response curves for Blatenská slat' illustrate significant relationships between primary and  
517 adventive pollen indicators and the AP:NAP ratio ( $p < 0.000202$ ), pollen richness ( $p < 0.00001$ ),  
518 pollen evenness ( $p < 0.0274$ ) and coprophilous fungi ( $p < 0.00278$ ) (Figure 5), sedimentation rates  
519 ( $p < 0.00104$ ) and the Ca/Zr ( $p < 0.00001$ ), Fe/Zr ( $p < 0.00001$ ) and Rb/Sr ratios ( $p < 0.00001$ )

520 (Figure 6). No significant relationships were found with the pioneer:successional ratio ( $p=0.116$ )  
521 (Figure 5), CHAR ( $p=0.474$ ), grass CHAR ( $p=0.209$ ), microCHAR ( $p=0.423$ ) (Figure 8), and  
522 herb CHAR ( $p=0.933$ ) (not shown). While not significant, a relationship trending towards  
523 significant was found between primary and adventive pollen indicators and wood CHAR  
524 ( $p=0.0619$ ) (not shown). The only significant relationships found between apophyte pollen  
525 indicators at Blatenská slat' were with AP:NAP ( $p<0.00001$ ), pioneer:successional ( $p<0.00431$ ),  
526 coprophilous fungi ( $p<0.0428$ ), pollen richness ( $p<0.00001$ ) (SI Figure 6), all geochemistry  
527 variables, Ca/Zr ( $p=0.00283$ ), Fe/Zr ( $p=0.00236$ ), Rb/Sr ( $p=0.000175$ ) and sedimentation rate  
528 ( $0.0404$ ) (SI Figure 7). No significant relationships were found between apophytes and pollen  
529 evenness ( $p<0.85$ ) (SI Figure 7), CHAR ( $p=0.615$ ), grass CHAR ( $p=0.54$ ), microCHAR  
530 ( $p=0.601$ ) (SI Figure 8), or herb CHAR ( $p=0.872$ ), and wood CHAR ( $p=0.488$ ) (not shown).

531

#### 532 **4.7 Principal Component Analysis**

533 For both sites, the PCA results based on selected pollen types and the total number of samples  
534 are shown in SI Figure 9 and 10. For Pěkná, the eigenvalues of the first two principal  
535 components were 9.52 and 6.8, respectively. The first and second principal components  
536 altogether accounted for 28.7% of the variance in fossil pollen assemblages. Taxa having large  
537 scores on PC1 are predominately primarily primary, adventive and apophyte pollen types.

538

539 For Blatenská slat', the eigenvalues of the first two principal components were 7.72 and 5.3,  
540 respectively. The first and second principal components altogether accounted for 24.3% of the  
541 variance in fossil pollen assemblages. Fossil pollen that corresponds with PC1 are mainly  
542 primary, adventive and apophyte pollen types.

543

### 544 **5 Discussion**

#### 545 ***5.1 Local wetland vegetation dynamics and establishment of testate amoebae records***

546 At Pěkná, at the onset of the record ~12,500 cal yr BP until ~9000 cal yr BP, macrofossils of  
547 several *Carex* taxa (*C. vesicaria*, *C. canescens*, *C. elata*, *C. rostrata*), and other wetland plants  
548 such as *Eriophorum vaginatum*, *Equisetum fluviatile*, *Filipendula ulmaria* and *Comarum*  
549 *palustre* (SI Figure 1) along with maximum Cyperaceae and Poaceae pollen percentages (SI  
550 Figure 5) indicate a tall-sedge marsh vegetation of Magno-Caricion elatae alliance. This alliance  
551 occupies the littoral zones of oligotrophic and mesotrophic water bodies where the water table is  
552 above the soil surface during most of the growing season (Šumberová et al. 2011). Magno-  
553 Caricion elatae alliance also represents the later stages in hydric succession of cut-off meanders  
554 within the floodplain of the Upper Vltava River (Buřková et al. 2005), suggesting that the Pěkná  
555 peat bog was originally an oxbow lake along the Upper Vltava River in the final stage of  
556 terrestrialization. High Rb/Sr, which is an indicator of erosion, suggests the oxbow lake was  
557 regularly influenced by local flooding until ~11,000 cal yr BP (Figure 3). High concentrations  
558 and percentages of pioneer species, such as *Pinus* sp. (likely *Pinus rotundata* and/or *P. sylvestris*  
559 based on modern vegetation assemblages) and *Betula pendula/pubescens* macrofossils and pollen



560 indicate both regional forestation and forestation of the peatland surface ~10,500 cal yr BP. Peat  
561 growth comprised primarily of *Eriophorum* peat coupled with wood fragments suggests a  
562 transition of a tall-sedge marsh into an oligotrophic groundwater-fed fen overgrown by trees  
563 starting ~10,500 cal yr BP and transitioning into peatbog shortly thereafter. As a result of peat  
564 formation, testate amoebae first appear ~10,500 cal yr BP (SI Figure 3), and thus provide a  
565 record of hydroclimate since ~10,500 cal yr BP at Pěkná (Figure 3). At Blatenská slat', the peat  
566 bog established ~7250 cal yr BP (Schafstall et al., 2024), which coincides with the first  
567 appearance of testate amoebae (SI Figure 4), thus providing a record of hydroclimate overlap  
568 between the two sites over the last ~7200 years.

569

## 570 ***5.2 Synchronous Holocene hydroclimate and forest succession, yet asynchronous fire regimes*** 571 ***across the Šumava Mountains***

572 Early Holocene hydroclimate reflects dry conditions above the modern agropastoral boundary  
573 Dreslerová et al., 2020a), likely in response to high summer insolation which induced warmer-  
574 and drier-than-present continental conditions (Berger and Loutre, 1991; Heiri et al., 2003;  
575 Fohlmeister et al., 2013) (Figure 3). This is further supported by the CHELSA model which  
576 shows the lowest precipitation values for the entire Holocene occurring between 12,000–8000  
577 cal yr BP. Additionally, the CHELSA simulated climate shows the warmest temperatures during  
578 the wettest quarter (i.e., summer) occurred between 10,000–8000 cal yr BP. This time period  
579 overlaps with the forestation of the Pěkná peatbog by early successional species *Pinus* and  
580 *Betula* (Figure 4). Modeled response curves illustrate local climate as the dominant driver of  
581 forest succession, with early pioneer species dominating when the water table is low (<20 cm)  
582 (Figure 5). Additionally, response curves show a significant relationship with local hydroclimate  
583 and landscape openness at Pěkná, with NAP dominating when the WTD is low. Moreover,  
584 authigenic Ca and Fe (Ca:Zr and Fe:Zr) increase ~10,500 cal yr BP suggesting the peatbog  
585 surface was seasonally dry and exposed to oxygen at this time (Figure 3). Modeled response  
586 curves illustrate strong relationships between WTDs and the Fe/Zr and Rb/Sr ratios (Figure 6),  
587 demonstrating hydroclimates influence on local peatbog surface dynamics. Warm and dry  
588 summer conditions coupled with a landscape dominated by early successional fire-adapted  
589 species resulted in more frequent biomass burning. For example, the first appearance of charred  
590 macrofossils, specifically charred bryophytes and wood, occurred around ~10,500 cal yr BP,  
591 with high concentrations of other charred macrofossils such as pine needles, leaves, moss, *Carex*  
592 and *Eriophorum* until ~7300 cal yr BP (Figure 7). GAM response curves further support a  
593 significant relationship between hydroclimate (WTD) and local biomass burning (charred  
594 macrofossils) (Figure 8). Additionally, the highest CHAR and microCHAR values of the entire  
595 record also occur between 11,000–7300 cal yr BP (Figure 7), with response curves illustrating a  
596 strong influence of hydroclimate on local and regional fire activity. Specifically, when WTDs are  
597 low, ranging between 15–25 cm, all charcoal-related variables drastically increase suggesting  
598 that when peat surface conditions are dry, the environment at Pěkná is especially prone to fire  
599 activity (Figure 8). The significant relationship between WTD and macrocharcoal, particularly

600 grass charcoal, supports the fact that fine fuels burned better under drier conditions (Turetski et  
601 al., 2014; Feurdean et al., 2022). Furthermore, macrocharcoal morphology data further support  
602 the charred macrofossil data in that both understory (herbs) and canopy (shrubs and wood) were  
603 burning, potentially indicating both low and high severity fires on the peat surface (Figure 7).  
604 High-severity fires are also inferred from the dramatic decrease in forest canopy pollen ~8,500  
605 cal yr BP (Figure 4), as well as by high concentrations of *Cenococcum geophilum*, a soil fungus  
606 that can be used as a proxy for soil erosion (Kroll, 1988), and an indicator of stress on vegetation  
607 as a result of chronic drought (Pigott, 1982; Coleman et al., 1989; Hasselquist et al., 2005)  
608 (Figure 7), as well as the presence of *Gelasinospora*, another soil fungus indicative of fire  
609 activity (van Geel, 1978). Interestingly, the highest peaks in CHAR occurred ~8000 cal yr BP,  
610 which is similar to other findings of high CHAR at this time (Carter et al., 2018a; Florescu et al.,  
611 *in review*). This supports other regional paleofire reconstructions that indicate high fire activity  
612 in the Šumava Mountains in the early Holocene (Carter et al., 2018a; Mateo-Beneito et al., 2024;  
613 Florescu et al., *in review*), Czechia (Bobek et al., 2019), and across Europe (Vannièrè et al.,  
614 2016; Feurdean et al., 2020). Similarly, Cagliero et al. (2023) also illustrate a positive  
615 relationship between climate (i.e., July temperature) and biomass burning in the Dinaric Alps  
616 supporting the strong influence of summer temperatures on fire activity. While the Blatenská slat'  
617 record does not extend beyond 7300 cal yr BP, the highest peaks in CHAR occurred at the onset  
618 of the record (Schafstall et al., 2024), further supporting regional burning across all elevations in  
619 the Šumava Mountains at this time (Figure 7).

620  
621 Starting ~7250 cal yr BP until 2200 cal yr BP, local hydroclimate records illustrate generally  
622 higher WTDs at both sites during this time, suggesting relatively cooler and wetter conditions  
623 overall, an inference supported by the CHELSA climate model which simulates cooler  
624 temperatures of the wettest quarter (Figure 3). However, WTDs do fluctuate indicating drought  
625 episodes and drying of the peat bog surfaces, which is supported by generally higher Ca/Zr  
626 and/or Fe/Zr at both sites until ~5500–4500 cal yr BP. Relatively synchronous responses in  
627 forest succession were recorded near the agropastoral boundary and at the highest elevations in  
628 the Šumava Mountains as a result of cooler and wetter conditions. Specifically, *Picea abies*  
629 dominated at both sites (Figure 4), which mirror other paleoecological reconstructions  
630 illustrating *P. abies* as the dominant forest canopy cover during the mid-Holocene (Svobodová et  
631 al., 2001, 2002; Carter et al., 2018a; Florescu et al., *in review*). Carter et al. (2018b) suggested  
632 that approximately 50% of the total land-cover across the entire Šumava Mountains was  
633 comprised of *P. abies* during the mid-Holocene. Our records suggest that higher elevations (i.e.,  
634 Blatenská slat', 1275 m asl) was comprised of ~75% *P. abies*, while mid-elevations (i.e., Pěkná,  
635 730 m asl) was comprised of ~40%. Increased forest density, low species richness and low  
636 evenness and wetter conditions coincided with *P. abies* dominance at both sites, indicating fewer  
637 species in the environment (Figure 5). Understory microclimates in *P. abies*-dominated forests  
638 are typically cooler, with abundant surface litter and acidic soils (Augusto et al., 2003;  
639 Colombaroli et al., 2012), which would impact pollen richness, particularly understory taxa in

640 these forested ecosystems (Figure 4). Modeled relationships further support the notion that  
641 regional forest succession and composition was climatically-driven between 7000–4000 cal yr  
642 BP.

643  
644 Because of cooler and wetter conditions, coupled with *P. abies* dominance, it would be expected  
645 that fire activity decreases as *P. abies* is a fire-avoidant species. However, *P. abies* establishment  
646 and rise to dominance in the Šumava Mountains occurred under elevated fire activity (Carter et  
647 al., 2018a). The rise to dominance of *P. abies* under elevated fire activity has also been witnessed  
648 in the Dinaric Alps (Cagliero et al., 2023) and Carpathians (Feurdean et al., 2012; Finsinger et  
649 al., 2018) suggesting a similar driver at the regional scale. At Pěkná, local fire activity is inferred  
650 from sporadic increases in charred macrofossils between 7700–4500 cal yr BP (Figure 3).  
651 Seasonally dry peatbog surfaces, which led to local fire activity at Pěkná, is supported by  
652 increased concentrations of *E. vaginatum* macrofossils and increased authigenic Ca. However,  
653 while increased authigenic Ca is also witnessed at Blatenská slat' between 7000–4000 cal yr BP,  
654 local fire activity essentially disappears from the record ~6000 cal yr BP. The synchronicity in  
655 forest composition points to climate as the primary driver, yet asynchronous fire regimes points  
656 to another ignition source (i.e. not climate) for fires at mid-elevations.

657  
658 *Picea abies* began to decrease at Pěkná starting ~5000 cal yr BP, likely because mean annual  
659 temperatures were too warm at this particular elevation (Figure 3). Mean annual temperatures  
660 may have reached a critical threshold ~4000 cal yr BP at higher elevations, which resulted in a  
661 drastic change in vegetation composition. Specifically, forests drastically changed from a *P.*  
662 *abies*-dominated forest to *Abies alba*-dominated forest at Blatenská slat', with higher pollen  
663 richness and slightly higher pollen evenness (Figure 4). The high proportion of *A. alba* at  
664 Blatenská slat' (~60%) are the first-ever reported at any site in the Šumava Mountains, which  
665 Schafstall et al. (2024) suggest may be a result of climate conditions becoming drier coupled  
666 with essentially no disturbance events in the surrounding environment. While a brief period of  
667 increased *Eriophorum vaginatum* ~4000 cal yr BP may suggest drier conditions locally (Figure  
668 3), the testate-derived hydroclimate does not illustrate any drastic decrease in WTDs ~4000 cal  
669 yr BP. In fact, WTDs continued to oscillate at higher values until ~2000 cal yr BP before  
670 decreasing to some of the lowest values recorded. We therefore propose that the increase in  
671 *Abies alba* was related to warming winter temperatures, likely spreading the species upslope  
672 from refuge from warmer temperatures at lower elevations. This assumption is based on the fact  
673 that temperate *Abies alba* is far more sensitive to winter frost and late frost than boreal *Picea*  
674 *abies* (Ellenberg, 2009; Lang et al., 2023).

675  
676 Local WTDs illustrate a major drought occurring between 2200–500 cal yr BP across the  
677 Šumava Mountains. WTDs decrease earlier at Blatenská slat' around ~2200 cal yr BP with  
678 consistently high percentages of *E. vaginatum* macrofossils indicating unstable hydrological  
679 conditions, whereas WTDs decrease ~1500 cal yr BP at Pěkná. The presence of *Calluna*

680 macrofossils further supports drier conditions at Pěkná over the last 1000 years (SI Figure 1). As  
681 a result of exceptionally dry conditions, similar to those witnessed in the early Holocene, forest  
682 density shifted to a more open landscape dominated by early pioneer species, which is supported  
683 by modeled response curves. *Picea abies* increases ~1000 cal yr BP at Blatenská slat' (Figure 4),  
684 likely in response to warmer temperatures (i.e. upslope migration). However, the Little Ice Age  
685 (LIA, 1450–1500 CE; Matthews and Briffa, 2005) does overlap with part of this time. Thus, the  
686 cool and wet LIA conditions may have favored *P. abies* growth (Grabner, 2017). Because of  
687 warm and exceptionally dry conditions, coupled with a landscape abundant with pioneer species,  
688 it would be expected that fire activity increases over the last 2000 years. Interestingly, we see a  
689 slight increase in CHAR at Blatenská slat' and decreasing CHAR at Pěkná (Figure 7). We  
690 speculate that the major drought witnessed between 2200–500 cal yr BP may have been  
691 primarily a winter-season drought, resulting in less snow at higher elevations. This may  
692 potentially explain why Blatenská slat' experienced slightly more fire activity than Pěkná due to  
693 fuels being drier-than-normal. Alternatively, these results may indicate that humans were  
694 primarily using fire at higher elevations. However, because no significant relationships were  
695 found between hydroclimate and any fire variable at Blatenská slat', this alludes to other factors  
696 being the primary driver behind the increase in fire activity at higher elevations over the last  
697 2000 years.

698

### 699 **5.3 How did human activities influence forest succession and composition?**

700 While hydroclimate has been the dominant driver of forest succession and composition, we  
701 cannot refute the possibility of humans as a secondary driver of landscape change. Archeological  
702 evidence documents human presence as early as the Mesolithic across the entire Šumava  
703 Mountain region (Fröhlich, 2003; Šída et al., 2011; Čuláková et al., 2012; Eigner et al., 2017;  
704 Kapustka et al., 2019; Kozáková et al., 2020), and near the vicinity of Pěkná (Vencl, 2006; Šída  
705 et al., 2008; 2012). Additionally, Blatenská slat' is located <1 km of an old Medieval route  
706 (Kozáková et al., 2020), which was important for trading salt, metals and other goods  
707 (Svobodová et al., 2001). At the mid-elevation site, Pěkná, both coprophilous fungi and  
708 adventive pollen indicators have been continuously present since ~4600 cal yr BP, which reflects  
709 livestock roaming on the landscape (Ptáková et al., 2021). Modeled response curves demonstrate  
710 a significant relationship between primary and adventive pollen indicators and coprophilous  
711 fungi, pollen evenness and pollen richness at (Figure 5), as well as apophyte pollen indicators  
712 and all forest succession/landscape openness variables (SI Figure 6). Over the last 3000 years,  
713 pollen richness (N0) has been slowly increasing at Pěkná in conjunction with a slow transition  
714 from a successional-dominated canopy to an early pioneer-dominated canopy (Figure 4). While  
715 the AP:NAP ratio suggests the landscape was still very much dominated by trees, pioneer taxa  
716 such as *Betula pubescens*, *Pinus sylvestris* and *P. rotunda* were increasing at this time. These  
717 taxa are more light-demanding than late-successional species like *Picea abies* (Beck et al., 2016;  
718 Houston Durrant et al., 2016), suggesting the landscape was not as dense as the AP:NAP ratio  
719 suggests. Macrofossil evidence further supports the relatively consistent presence of *Pinus* on the

720 Pěkná peatbog since ~4000 cal yr BP (SI Figure 1). Regular grazing would have maintained an  
721 intermediate state between open pasture and closed woodland, typical of a woodland pasture  
722 environment (Vera, 2000; Hartel et al. 2015). This intermediate state would have favored  
723 understory herb and shrub growth beneficial for grazers. These results suggest that the Vltava  
724 River floodplain near Pěkná was likely frequently visited by grazers, which likely attracted  
725 hunters, should these have been wild game instead of domesticated livestock. However, if these  
726 were domesticated livestock, either scenario points to human presence. Additionally, the  
727 proximity to the Vltava River would have been beneficial for human occupation not only for  
728 mobility purposes, but also easy access to water and food. Increases in adventive pollen  
729 indicators overlap with the first appearance, and continued presence of primary pollen indicators  
730 including cultivars ~1450 cal yr BP (Figure 4). This suggests that humans were beginning to  
731 utilize agropastoral farming near Pěkná, which is ~100 m upslope from the modern-day  
732 agropastoral farming boundary (Dreslerová et al., 2020a). Increasing Pb/Zr over the last 2000  
733 years is likely associated with the regional mining of ore (Veron et al., 2014) (Figure 3). Forests  
734 in the Šumava Mountains were used for charcoal and potash production for local iron smelters in  
735 the 16<sup>th</sup> century (Veselý et al., 1993), and glassworks in the 14<sup>th</sup> century (Fröhlich, 2003). Pb as  
736 well as Cu and Co are common colorant elements used in glassworks, especially blue glassworks  
737 (Bidegaray and Pollard, 2018; Zlámálová Cílová et al., 2021) which were popular glassworks for  
738 the region. Starting ~1200 cal yr BP, evidence of human activities directly modifying the local  
739 environment is evident in the Pěkná record, with a relatively large increase in primary and  
740 adventive pollen indicators (Figure 4). This overlaps with the pioneer:successional ratio  
741 illustrating more early pioneer taxa on the landscape. The largest ecosystem change has occurred  
742 over the last 500 years, with the decline of *Abies alba* at Pěkná likely associated with  
743 deforestation (Kolář et al., 2021). The large increase in NAP over the last 500 years illustrates a  
744 growing demand of agriculture and pasture area at lower elevations.

745  
746 While we hypothesized human impact would be greater at Pěkná due to its proximity to the  
747 modern-day agropastoral farming boundary, surprisingly, we found comparable evidence of  
748 human impact at Blatenská slat'. Similar to Pěkná, adventive pollen indicators have been  
749 consistently present since ~4250 cal yr BP suggesting human utilization of high elevation forests.  
750 Modeled response curves demonstrate that a more open landscape with higher NAP species and  
751 pollen richness is associated with higher primary and adventive human indicator pollen (Figure  
752 5) and apophyte pollen indicators at Blatenská slat' (SI Figure 6). Two time periods with higher  
753 NAP species and pollen richness occurred, first between 4000–2000 cal yr BP and then over the  
754 last 1000 years. During each of these periods, a similar environmental scenario that occurred at  
755 Pěkná also occurred at Blatenská slat'. For example, pollen richness (N0) was exceptionally high  
756 during these two time periods, with rapid fluctuations in the pioneer:successional ratio  
757 suggesting a mixture of each forest type. While not significant, there appears to be a relationship  
758 trending towards significant with human activities and both the pioneer:successional ratio  
759 ( $p=0.07280$ ), and coprophilous fungi ( $p=0.074$ ). The modeled relationships between human

760 pollen indicator taxa, pollen richness and coprophilous potentially point to an environment with a  
761 higher mosaic of species richness that would have been favorable for gathering seasonally  
762 ethnobotanically important species found at higher elevations. Additionally, the potentially semi-  
763 open woodland may have been favorable for seasonal pastoralism. While we cannot say for  
764 certain that the time period between 4000–2000 cal yr BP with higher pollen richness and  
765 landscape openness was attributed directly to human influence, we can speculate that humans  
766 were utilizing resources at higher elevations during this period. However, there is more  
767 circumstantial evidence suggesting direct human impact at higher elevations over the last 1000–  
768 500 years. Notably, the drastic increase in Pb/Zr and primary indicator pollen taxa point to direct  
769 human influence in the region. Additionally, the drastic increase in *Picea abies* over the last  
770 1000 years may have been a result of human management. Specifically, historical timber  
771 construction in the present-day Czech Republic included *P. abies* and *Abies alba* (Kolář et al.,  
772 2021). Starting in the mid-17<sup>th</sup> century onward, but perhaps as early as the end of the 14<sup>th</sup> century  
773 (e.g. in southern Germany), *Picea abies* was likely planted across the study region due to  
774 increasing construction demand (cf. Hölzl, 2010; Antoine et al., 2024). Additionally, *Picea abies*  
775 has also been shown to benefit from grazing and browsing (Ellenberg, 2009; Rey et al., 2013;  
776 Schwörer et al., 2015; Lang et al., 2023). Our results indeed illustrate the consistent presence of  
777 *Sporormiella* over the last 500 years which may have contributed to the recent expansion of *P.*  
778 *abies* (Figure 4). Deforestation at higher elevations likely increased local weathering of the  
779 Blatenská slat' catchment over the last 1000 years, as indicated by increasing Rb/Sr (Figure 3).  
780 Modeled response curves demonstrate a significant relationship between primary and adventive  
781 pollen indicator taxa and the Rb/Sr ratio (Figure 6). Lastly, the decrease in forest cover and  
782 decline in pollen evenness over the last 1000 years supports previous quantitative REVEALS  
783 land-cover reconstructions which illustrate increasing landscape openness, especially over the  
784 last 500 years (Carter et al., 2018b). These data contribute to the growing body of literature  
785 illustrating how human deforestation has impacted vegetation composition and diversity over  
786 time (Antoine et al., 2024).

787

#### 788 **5.4 What drove the observed asynchronous changes in fire activity?**

789 Approximately 96% of all modern wildfires in the European Union are caused by humans, which  
790 are being exacerbated by recent climate change (European Commission Joint Research Centre,  
791 2023). Historic fires were likely also dominated by human ignition sources for pastoral purposes  
792 across Europe and in the Šumava Mountains. However, pastoral fires in the Šumava Mountains  
793 are unlikely to be detected by anthropogenic indicators, likely because there is a lack of pollen or  
794 spore evidence for pastoralism in this region (Kozáková et al., 2020). As such, modeled response  
795 curves do not show a relationship between primary and adventive pollen indicators, apophyte  
796 pollen indicators, and any fire variable. Instead GAM response curves illustrate a strong positive  
797 relationship between hydroclimate and every fire variable at Pěkná (Figure 8). However, this  
798 could be an artifact of the GAMs, as there are fewer observations using the sum of primary and  
799 adventive pollen indicator taxa as the predictor variable than the number of testate amoebae

800 observations as the predictor variables (see vertical dashed lines on GAMS x-axes; Figures 5, 6  
801 and 8).

802

803 It was likely that humans were utilizing fire, but not enough to override climate as the dominant  
804 driver of fire. This is supported by local paleofire lacustrine-based reconstructions that document  
805 an increase in fire frequency in response to human occupation (Carter et al., 2018a; Florescu et  
806 al., *in review*). Lacustrine-based paleofire records are likely more reflective of regional activity,  
807 whereas peatbog-based paleofire records are more localized. Therefore, without direct  
808 archeological evidence documenting the physical presence of humans at Pěkná and Blatenská  
809 slat', the likelihood of finding any anthropogenically-related fire signal decreases, as does that  
810 ability to create a realistic estimate of population size of prehistoric communities from the area,  
811 which is a current challenge in the field of archeology (Kolář et al., 2022). Other studies from  
812 Europe have demonstrated the ability of humans to override climate as the primary driver of fire  
813 activity (e.g. Rey et al., 2013; 2019). However, these studies come from the Alps where the use  
814 of fire to create or maintain high-altitude pastures has been well documented (Pini et al., 2017;  
815 Gilck and Poschlod, 2019; Dietre et al., 2020). As Kozáková et al. (2020) suggest, the absence of  
816 a treeless zone in Šumava Mountains makes it more challenging to identify pastoral fires or other  
817 human-fire related activities. Such inferences showing a close link between land use and fire  
818 may depend on different climatic, vegetational and cultural settings as well as the sufficient  
819 preservation or investigation of the archeological remains. For example, Carter et al. (2021)  
820 showed that humans overrode climate as the dominant driver of fire in a high-elevation fire-  
821 prone mixed-conifer forest in south-central Utah, USA. Specifically, they showed that a 600-year  
822 period of elevated CHAR was associated with the farming-based Fremont culture, who likely  
823 used frequent, low-severity fire to increase plant resources beneficial for human usage. Because  
824 that specific study site had onsite archeological evidence (i.e., hearths), the odds of identifying a  
825 human-fire signature increased substantially. Additionally, the high prevalence of radiocarbon-  
826 dated archeological sites surrounding their study site allowed for creating a summed probability  
827 distribution (SPDs) which was used to distinguish human-caused fires from naturally caused  
828 ones. However, we acknowledge that the climate, vegetation, and fire regimes vary substantially  
829 between south-central Utah, USA (Carter et al., 2021) and Central Europe (this study or the  
830 Alps).

831

## 832 **Conclusions**

833 Documenting prehistoric human impact in Central European mountain environments has been a  
834 challenge. However, our study has demonstrated that long-term human impacts have left legacy  
835 effects on modern forest succession in central European mountain environments. By presenting  
836 the first records of reconstructed water table depths (WTDs) from the Šumava Mountains, our  
837 study demonstrated that major changes in forest succession primarily resulted from climate. Yet  
838 humans likely played a secondary role in modifying forest succession to increase resources  
839 beneficial to both humans and grazers over the last ~4600 years. However, the influence of

840 human activities in modifying forest succession increased substantially over the past 1000 years  
841 at both sites. We expected to see a larger anthropogenic footprint at Pěkná, as there is a higher  
842 prevalence of human settlements nearby. However, we found comparable evidence of human  
843 impact at Blatenská slat', especially over the last 1000 years. We were unable to document the  
844 use of fire as a tool to manipulate landscapes, and that the main driver of local and regional fire  
845 is climate. Our inability to provide direct evidence of people utilizing fire as a landscape  
846 management tool may be attributed to the lack of archeological evidence documenting human  
847 habitation at Pěkná and Blatenská slat' or to local settings (e.g. lacking natural grasslands at  
848 higher elevations, humid conditions preventing large-scale burning, a lack of flammable  
849 vegetation, or the more localized nature of peatbog records versus regional-scale lacustrine  
850 records). Additional archeological evidence and sedimentary DNA data from the Šumava  
851 Mountains are desperately needed to better disentangle humans' role in altering vegetation  
852 assemblages and fire regimes prior-to the High Middle Ages.

853

#### 854 **Acknowledgements**

855 We would like to thank Vojtěch Abraham and Jan Šašek for their help in the field at Pěkná, and  
856 Daniel Vondrák and Nick Schafstall for their help in the field at Blatenská slat'. Additionally, we  
857 would like to thank Viktor Goliáš for his contribution on <sup>210</sup>Pb dating. This project was funded  
858 by the Czech Science Foundation, BOBAFIRES project #19-14271Y and BESTFORCE project  
859 #20-13368S, by Masaryk University project MUNI/A/1323/2022, by RES-HUM -  
860 CZ.02.01.01/00/22\_008/0004593 (MEYS + EU), and by the Laboratory Directed Research and  
861 Development program at Los Alamos National Laboratory under project number  
862 20230864PRD3.

863

#### 864 **References:**

- 865 1. Amesbury, M.J., Swindles, G.T., Bobrov, A., Charman, D.J., Holden, J., Lamentowicz, M.,  
866 Mallon, G., Mazei, Y., Mitchell, E.A.D., Payne, R.J., Roland, T.P., Turner, T.E., Warner,  
867 B.G., 2016. Development of a new pan-European testate amoeba transfer function for  
868 reconstructing peatland palaeohydrology. *Quaternary Science Reviews* 152, 132–151,  
869 <https://doi.org/10.1016/j.quascirev.2016.09.024>.
- 870 2. Antoine, E., Marquer, L., Muigg, B., Tegel, W., Bisson, U., Bolliger, M., Herzig, FF.,  
871 Heussner, K.-U., Hofmann, J., Kontic, R., Kyncl, T., Land, A., Lechterbeck, J., Leuschner,  
872 H.H., Linderholm, H.W., Neyses-Eiden, M., Rösch, M., Rzepecki, A., Walder, F.,  
873 Weidemüller, J., Seim, A. 2024. Legacy of last millennium timber use on plant cover in  
874 Central Europe: Insights from tree rings and pollen. *Science of the Total Environment* 922,  
875 171157, <https://doi.org/10.1016/j.scitotenv.2024.171157>.
- 876 3. Augusto, L., Dupouey, J.-L., Ranger, J. 2003. Effects of tree species on understory  
877 vegetation and environmental conditions in temperate forests. *Annals of Forest Science* 60,  
878 823–831, <https://doi.org/10.1051/forest:2003077>.



- 879 4. Baker, A.G., Bhagwat, S.A., Willis, K.J., 2013. Do dung fungal spores make a good proxy  
880 for past distribution of large herbivores? *Quaternary Science Reviews* 62, 21–31,  
881 <https://doi.org/10.1016/j.quascirev.2012.11.018>
- 882 5. Behre, K.-E. 1981. The interpretation of anthropogenic indicators in Pollen Diagrams.  
883 *Pollen Spores*, 23, 225–245.
- 884 6. Behre, K.-E. 1988. The role of man in European vegetation history. In: Huntley, B., Webb,  
885 T. (Eds.) *Vegetation History. Handbook of Vegetation Science*, Springer, Dordrecht, 633672,  
886 [https://doi.org/10.1007/978-94-009-3081-0\\_17](https://doi.org/10.1007/978-94-009-3081-0_17).
- 887 7. Behre, K.-E., van der Knapp, W.O., Lang, G., Morales-Molino, C., Tinner, W. In:  
888 *Anthropogenic changes to vegetation*, Lang, G., Ammann, B., Behre, K.-E., Tinner, W.  
889 (Eds). 2023, pp. 363–408.
- 890 8. Beck, P., Caudullo, G., de Rigo, D., Tinner, W. 2016. *Betula pendula*, *Betula pubescens* and  
891 other birches in Europe: distribution, habitat, usage and threats. In: San-Miguel Ayanz, J., de  
892 Rigo, D., Caudullo, G., Houston Durrant, T., Mauri, A. (Eds.) *European Atlas of Forest Tree*  
893 *Species*. Publi. Off. EU, Luxembourg, pp. e010226+.
- 894 9. Berger, A., and Loutre, M.F., 1991. Insolation value for the climate of the last 10 million 775  
895 years. *Quaternary Science Reviews* 10, 297–317, [https://doi.org/10.1016/0277-](https://doi.org/10.1016/0277-3791(91)90033-Q)  
896 [3791\(91\)90033-Q](https://doi.org/10.1016/0277-3791(91)90033-Q).
- 897 10. Beug, H.-J. 2004. *Leitfaden der Pollenbestimmung für Mitteleuropa und angrenzende*  
898 *Gebiete*. Verlag Dr Friedrich Pfeil, Munich.
- 899 11. Bidegaray, A.-I., and Pollard, A.M. 2018. Tesserae Recycling in the Production of Medieval  
900 Blue Window Glass. *Archaeometry* 60, 784–796, <https://doi.org/10.1111/arcm.12350>
- 901 12. Birks, H.J.B., Line, J.M. 1992. The use of rarefaction analysis for estimating palynological  
902 richness from Quaternary pollen-analytical data. *The Holocene*, 2, 1–10,  
903 <https://doi.org/10.1177/095968369200200101>.
- 904 13. Birks, H.H., 2007. Plant macrofossil introduction. In: Elias, S.A. (Ed.), *Encyclopedia of*  
905 *Quaternary Science*, vol. 3. Elsevier, Amsterdam, pp. 2266–2288.
- 906 14. Birks, H.J.B., Felde, V.A., Bjune, A.E., Grytnes, J.-A., Seppä, H., Giesecke, T. 2016. Does  
907 pollen-assemblage richness reflect floristic richness? A review of recent developments and  
908 future challenges. *Review of Palaeobotany and Palynology*, 228, 1–25,  
909 <https://doi.org/10.1016/j.revpalbo.2015.12.011>.
- 910 15. Blaauw, M., and Christeny, J.A., 2011. Flexible paleoclimate age-depth models using an  
911 autoregressive gamma process. *Bayesian Analysis* 6, 457–474. [https://doi.org/10.1214/11-](https://doi.org/10.1214/11-BA618)  
912 [BA618](https://doi.org/10.1214/11-BA618).
- 913 16. Blackford, J.J., 2000. Palaeoclimatic records from peat bogs. *Trends in Ecology and*  
914 *Evolution*. 15, 193–198, [https://doi.org/10.1016/S0169-5347\(00\)01826-7](https://doi.org/10.1016/S0169-5347(00)01826-7)
- 915 17. Bobek, P., Svobodová-Svitavská, H., Pokorný, P., Šamonil, P., Kuneš, P., Kozáková, R.,  
916 Abraham, V., Klinerová, T., Gabriela Švarcová, M., Jamrichová, E., Krauseová, E., Wild, J.  
917 (2019). Divergent fire history trajectories in Central European temperate forests revealed a

- 918 pronounced influence of broadleaved trees on fire dynamics. *Quaternary Science Reviews*  
919 225, 105865, <https://doi.org/10.1016/j.quascirev.2019.105865>.
- 920 18. Bojňanský, V and Fargašová, A. 2007. *Atlas of Seeds and Fruits of Central and East-*  
921 *European Flora* Springer, Dordrecht, The Netherlands.
- 922 19. Boyle, J.F. 2001. Inorganic geochemical methods in paleolimnology. In: Last W, Smol JP  
923 (Eds.) *Tracking environmental change using lake sediments, physical and geochemical*  
924 *methods*. Kluwer, Dordrecht, pp 83–142.
- 925 20. Bufková, I., Prach, K., Bastl, M. 2005. Relationship between vegetation and environment  
926 within the montane flood plain of the Upper Vltava River (Šumava National Park, Czech  
927 Republic). *Silva Gabreta*, 2, 5–76.
- 928 21. Cagliero, E., Paradis, L., Marchi, N., Lisztes-Szabó, Z., Braun, M., Hubay, K., Sabatier, P.,  
929 Čurovič, M., Spalevic, V., Motta, R., Lingua, E, Finsinger, W. 2023. The role of fire  
930 disturbances, human activities and climate change for long-term forest dynamics in upper-  
931 montane forests of the central Dinaric Alps. *The Holocene* 33(7), 827–841,  
932 <https://doi.org/10.1177/09596836231163515>.
- 933 22. Carter, V.A., Moravcová, A., Chiverrell, R.C., Clear, J.L., Finsinger, W., Dreslerová, D.,  
934 Halsall, K., Kuneš, P. 2018a. Holocene-scale fire dynamics of central European temperate  
935 spruce-beech forests. *Quaternary Science Reviews* 191, 15–30,  
936 <https://doi.org/10.1016/j.quascirev.2018.05.001>.
- 937 23. Cappers, R.T.J., Bekker, R.M., Jans, J.E.A. 2006. *Digitale Zadenatlas Van Nederland*  
938 *Barkhuis Publishers, Groningen*.
- 939 24. Carter, V.A., Chiverrell, R.C., Clear, J.L., Kuosmanen, N., Moravcová, A., Svoboda, M.,  
940 Svobodová-Svitavská, H., van Leeuwen, J.F.N., van der Knapp, W.O., Kuneš, P. 2018b.  
941 *Quantitative Palynology Informing Conservation Ecology in the Bohemian/Bavarian Forests*  
942 *of Central Europe*. *Frontiers in Plant Science* 8, 2268,  
943 <https://doi.org/10.3389/fpls.2017.02268>.
- 944 25. Carter, V.A., Bobek, P., Moravcová, A., Šolcová, A., Chiverrell, R.C., Clear, J.L., Finsinger,  
945 W., Feurdean, A., Tanțău, I., Magyari, E., Brussel, T., Kuneš, P. 2020. The role of climate-  
946 fuel feedbacks on Holocene biomass burning in upper-montane Carpathian forests. *Global*  
947 *and Planetary Change* 193, 103264, <https://doi.org/10.1016/j.gloplacha.2020.103264>.
- 948 26. Carter, V.A., Brunelle, A., Power, M.J., DeRose, R.J., Bekker, M., Hart, I., Brewer, S.,  
949 Spangler, J., Robinson, E., Abbott, M., Maezumi, S.Y., Coddling, B.F. 2021. Legacies of  
950 Indigenous land use shaped past wildfire regimes in the Basin-Plateau Region, USA.  
951 *Communications Earth and Environment* 2, 72, <https://doi.org/10.1038/s43247-021-00137-3>.
- 952 27. Chen, J., An, Z., Head, J., 1999. Variation of Rb/Sr ratios in the Loess-paleosol sequences of  
953 central China during the last 130,000 years and their implications for monsoon  
954 paleoclimatology. *Quaternary Research* 51, 215–219. <https://doi.org/10.1006/qres.1999.2038>.
- 955 28. Coleman, M.D., Bledsoe, C.S., Lopushinsky, W. 1989. Pure culture response of  
956 ectomycorrhizal fungi to imposed water stress. *Canadian Journal of Botany*, 67, 29–39,  
957 <https://doi.org/10.1139/b89-005>.

- 958 29. Colombaroli, D., Beckmann, M., van der Knapp, W.O., Curdy, P., Tinner, W. 2012. Changes  
959 in biodiversity and vegetation composition in the central Swiss Alps during the transition  
960 from pristine forest to first farming. *Biodiversity Research* 19, 157–170,  
961 <https://doi.org/10.1111/j.1472-4642.2012.00930.x>.
- 962 30. Čuláková, K., Eigner, J., Metlička, M., Přichystal, A. and Řezáč, M. 2012. Horské  
963 mezolitické osídlení u Javoří pily, obec Modrava, okres Klatovy. *Archeologie ve středních*  
964 *Čechách* 16, 19–28.
- 965 31. Deza-Araujo, M., Morales-Molino, C., Tinner, W., Henne, P.D., Heitz, C., Pezzatti, G.B.,  
966 Hafner, A., Conedera, M. 2020. A critical assessment of human-impact indices based on  
967 anthropogenic pollen indicators. *Quaternary Science Reviews* 236, 106291,  
968 <https://doi.org/10.1016/j.quascirev.2020.106291>.
- 969 32. Dietre, B., Reitmaier, T., Walser, C., Warnk, T., Unkel, I., Hajdas, I., Lambers, K., Reidl, D.,  
970 Nicolas Hass, J. 2020. Steady transformation of primeval forest into subalpine pasture during  
971 the Late Neolithic to Early Bronze Age (2300–1700 BC) in the Silvretta Alps, Switzerland.  
972 *The Holocene* 30(3), 355–368, <https://doi.org/10.1177/0959683619887419>.
- 973 33. Dreslerová, D., Romportl, D., Čišecký, Č., Fröhlich, J., Michálek, J., Metlička, M., Parkman,  
974 M., Pták, M., 2020a. At the end of the world? Settlement in the Šumava mountains and  
975 foothills in later prehistory. *Praehistorische Zeitschrift* 95, 1–23, [https://doi.org/10.1515/pz-](https://doi.org/10.1515/pz-2021-0019)  
976 [2021-0019](https://doi.org/10.1515/pz-2021-0019).
- 977 34. Dreslerová, D., Kozáková, R., Metlička, M., Brychová, V., Bobek, P., Čišecký, Č., Demján,  
978 P., Lisá, L., Pokorná, A., Michálek, J., Strouhalová, B., Trubač, J., 2020b. Seeking the  
979 meaning of a unique mountain site through a multidisciplinary approach. *The Late La Tène*  
980 *site at Sklářské Valley, Šumava Mountains, Czech Republic. Quaternary International* 542,  
981 88–108, <https://doi.org/10.1016/j.quaint.2020.03.013>.
- 982 35. Dreslerová, D., Venclová, N., Demján, P., Kyselý, R., Matoušek, V., 2022. Did they leave or  
983 not? A critical perspective on the beginnings of the La Tène period in Bohemia.  
984 *Archaeologické rozhledy* 74, 505–537, <https://doi.org/10.35686/AR.2022.24>.
- 985 36. Eigner, J., Kapustka, K., Parkman, M., Řezáč, M. 2017. Mezolitické osídlení Šumavy  
986 pohledem studia surovin kamenných artefaktů z lokalit Javoří Pila 1 a Nova Pec [Mesolithic  
987 occupation of the Bohemian Forest according to the study of raw materials for lithic  
988 production from the sites of Javoří Pila 1 and Nova. *Silva Gabreta* 23, 33–44.
- 989 37. Ellenberg, H., 2009. *Vegetation Ecology of Central Europe*, 4th ed. Cambridge University  
990 Press, Cambridge.
- 991 38. Enache, M.D., Cumming, B.F., 2006. Tracking recorded fires using charcoal morphology  
992 from the sedimentary sequence of Prosser Lake, British Columbia (Canada). *Quaternary*  
993 *Research* 65, 282–292, <https://doi.org/10.1016/j.yqres.2005.09.003>.
- 994 39. Engstrom, D.R., Wright, H.E., Jr 1984. Chemical stratigraphy of lake sediments as a record  
995 of environmental change. In: Haworth EY, Lund JWG (Eds.) *Lake sediments and*  
996 *environmental history*. Leicester University Press, Leicester, pp 11–68.

- 997 40. European Commission, Joint Research Centre, San-Miguel-Ayanz, J., Durrant, T., Boca, R.  
998 2023. Forest fires in Europe, Middle East and North Africa 2022, Publications Office of the  
999 European Union. <https://data.europa.eu/doi/10.2760/348120>.
- 1000 41. Faegri, K., Kaland, P.E., and Krzywinski, 1989. Textbook of Pollen Analysis. Wiley, New  
1001 York.
- 1002 42. Feurden, A., Spessa, A., Magyari, E.K., Willis, K.J., Veres, D., Hickler, T. 2012. Trends in  
1003 biomass burning in the Carpathians region over the last 15,000 years. *Quaternary Science*  
1004 *Reviews* 45, 111–125, <https://doi.org/10.1016/j.quascirev.2012.04.001>.
- 1005 43. Feurdean, A., Gałka, M., Tanțău, I., Geantă, A., Hutchinson, S.M., Hickler, T. 2016. Tree  
1006 and timberline shifts in the northern Romanian Carpathians during the Holocene and the  
1007 response to environmental changes. *Quaternary Science Reviews* 134(15), 100–113,  
1008 <https://doi.org/10.1016/j.quascirev.2015.12.020>.
- 1009 44. Feurdean, A., Florescu, G., Vanni ere, B., Tanțău, I., O’Hara, R.B., Pfeiffer, M., Hutchinson,  
1010 S.M., Gałka, M., Moskal-del Hoyo, M., Hickler, T., 2017. Fire has been an important driver  
1011 of forest dynamics in the Carpathian Mountains during the Holocene. *Forest Ecology and*  
1012 *Management* 389, 15–26, <https://doi.org/10.1016/j.foreco.2016.11.046>.
- 1013 45. Feurdean, A. Vasiliev, I. 2019. The contribution of fire to the late Miocene spread of  
1014 grasslands in eastern Eurasia (Black Sea region). *Scientific Reports* 9, 6750,  
1015 <https://doi.org/10.1038/s41598-019-43094-w>.
- 1016 46. Feurdean, A., Vanni ere, B., Finsinger, W., Warren, D., Connor, S.C., Forrest, M., Liakka, J.,  
1017 Panait, A., Werner, C., Andri , M., Bobek, P., Carter, V.A., Davis, B., Diaconu, A.-C.,  
1018 Dietze, E., Feeser, I., Florescu, G., Gałka, M., Giesecke, T., Jahns, S., Jamrichova, E.,  
1019 Kajukało, K., Kaplan, J., Karpińska-Ko aczek, M., Ko aczek, P., Kuneš, P., Kupriyanov, D.,  
1020 Lamentowicz, M., Lemmen, C., Magyari, E.K., Marcisz, K., Marinova, E., Niamir, A.,  
1021 Novenko, E., Obremaska, M., Pędziszewska, A., Pfeiffer, M., Poska, A., R sch, M.,  
1022 Słowiński, M., Stan ikait , M., Szal, M., Świ ta-Musznicka, J., Tanțău, I., Theuerkauf, M.,  
1023 Tonkov, S., Valk , O., Vassiljev, J., Veski, S., Vincze, I., Wacnik, A., Wiethold, J., Hickler  
1024 T. 2020. Fire hazard modulation by long-term dynamics in land cover and dominant forest  
1025 type in eastern and central Europe. *17*(5), 1213–1230, [https://doi.org/10.5194/bg-17-1213-](https://doi.org/10.5194/bg-17-1213-2020)  
1026 [2020](https://doi.org/10.5194/bg-17-1213-2020).
- 1027 47. Feurdean, A., Diaconu, A.-C., Pfeiffer, M., Gałka, M., Hutchinson, S.M., Butiseaca, G.,  
1028 Gorina, N., Tonkov, S., Niamir, A., Tanțău, I., Zhang, H., Kirpotin, S. 2022. Holocene  
1029 wildfire regimes in western Siberia: interaction between peatland moisture conditions and the  
1030 composition of plant functional types. *Climate of the Past* 18(6), 1255–1274,  
1031 <https://doi.org/10.5194/cp-18-1255-2022>.
- 1032 48. Finsinger, W., and Tinner, W. 2005. Minimum count sums for charcoal-concentration  
1033 estimates in pollen slides: accuracy and potential errors. *The Holocene* 15(2), 293–297,  
1034 <https://doi.org/10.1191/0959683605hl808rr>.
- 1035 49. Finsinger, W., Morales-Molino, C., Gałka, M., Valsecchi, V., Bojovic, S., Tinner, W. 2017.

- 1036 Holocene vegetation and fire dynamics at Crveni Potok, a small mire in the Dinaric Alps  
1037 (Tara National Park, Serbia). *Quaternary Science Reviews* 167, 63–77,  
1038 <http://dx.doi.org/10.1016/j.quascirev.2017.04.032>.
- 1039 50. Finsinger, W., Fevre, J., Orbán, I., Pál, I., Vincze, I., Hubay, K., Birks, H.H., Braun, M.,  
1040 Tóth, M., Magyari, E.K. 2018. Holocene fire-regime changes near the treeline in the Retezat  
1041 Mountains. (Southern Carpathians, Romania). *Quaternary International* 477(30), 94–105,  
1042 <https://doi.org/10.1016/j.quaint.2016.04.029>.
- 1043 51. Fröhlich, J. 2003. Sklářství Šumavy (*Glass-making in Šumava*). In: Šumava. Příroda,  
1044 historie, život. Baset, pp 1–799.
- 1045 52. Florescu, G., Tinner, W., Feurdean, A., Finsinger, W., Kuneš, P., Vondrák, D., Heurich, M.,  
1046 van der Knaap, P., Kletetscka, G., Kraklow, V. (in review). Forest composition and density  
1047 shaped long-term fire regimes and lake-catchment interactions in the Bavarian mountain  
1048 temperate mixed forests, Central Europe.
- 1049 53. Florescu, G., Hutchinson, S.M., Gałka, M., Mîndrescu, M., Tantău, I., Petras, A., Feurdean,  
1050 A. 2024. The legacy of millennial-scale land-use practices on landscape composition,  
1051 diversity and slope erosion in the subalpine areas of Eastern Carpathians, Romania. *The*  
1052 *Holocene* 34(4), 467–486, <https://doi.org/10.1177/09596836231219473>.
- 1053 54. Fohlmeister, J., Vollweiler, N., Spötl, C., Mangini, A., 2013. COMNISPA II: Update of a  
1054 931 mid-European isotope climate record, 11 ka to present. *The Holocene* 23(5), 749–754.  
1055 doi: 932 10.1177/0959683612465446.
- 1056 55. Geantă, A., Gałka, M., Tanțău, I., Hutchinson, S.M., Mîndrescu, M., Feurdean, A. 2014.  
1057 High mountain region of the Northern Romanian Carpathians responded sensitively to  
1058 Holocene climate and land use changes: A multi-proxy analysis. *The Holocene* 24(8), 944–  
1059 956, <https://doi.org/10.1177/0959683614534747>.
- 1060 56. Grabner, M. 2017. Werkholz: Eigenschaften und historische Nutzung 60 mitteleuropäischer  
1061 Baum- und Straucharten. Verlag Dr. Kessel, Remagen-Oberwinter.
- 1062 57. Grimm, E.C. 2004. TILIA and TGView. Springfield: Illinois State Museum, Research and  
1063 Collection Center.
- 1064 58. Gilck, F., and Poschlod, P., 2019. The origin of alpine farming: A review of archaeological,  
1065 linguistic and archaeobotanical studies in the Alps. *The Holocene* 29, 1503–1511,  
1066 <https://doi.org/10.1177/0959683619854511>.
- 1067 59. Hafner, A., Schworer, C., 2018. Vertical mobility around the high-alpine Schnidejoch Pass.  
1068 Indications of Neolithic and Bronze Age pastoralism in the Swiss Alps from paleoecological  
1069 and archaeological sources. *Quaternary International* 484, 3–18,  
1070 <https://doi.org/10.1016/j.quaint.2016.12.049>.
- 1071 60. Hammer, O., Harper, D.A.T., Ryan, D. 2001. PAST: Paleontological Statistics Software  
1072 Package for Education and Data Analysis. *Palaeontologia Electronica* 4(1), 1–9.
- 1073 61. Hartel, T., Plieninger, T., Varga, A. 2015 Wood-pastures in Europe. In: Kirby KJ, Watkins C  
1074 (Eds.) *Europe's changing woods and forests: from wildwood to managed landscapes*. CABI  
1075 Publishing, Wallingford, pp 61–76.

- 1076 62. Hasselquist, N., Germino, M.J., McGonigle, T., Smith, W.K. 2005. Variability of  
1077 Cenococcum colonization and its ecophysiological significance for young conifers at alpine–  
1078 treeline. *New Phytologist* 165, 867–873, doi: 10.1111/j.1469-8137.2005.01275.x.
- 1079 63. Hastie, T.J., and Tibshirani, R.J., 1986. Generalized Additive Models. *Statistical Science*  
1080 1(3), 297–318, <https://www.jstor.org/stable/2245459>.
- 1081 64. Heiri, O., Lotter, A.F., Hausmann, S., Kienast, F. 2003. A chironomid-based Holocene  
1082 summer air temperature reconstruction from the Swiss Alps. *The Holocene* 13, 477–484,  
1083 <https://doi.org/10.1191/0959683603hl640ft>.
- 1084 65. Hendon, D., and Charman, D.J., 1997. The preparation of testate amoebae (Protozoa:  
1085 rhizopoda) samples from peat. *The Holocene* 7, 199–205, [https://doi.org/10.1177/](https://doi.org/10.1177/095968369700700207)  
1086 [095968369700700207](https://doi.org/10.1177/095968369700700207).
- 1087 66. Henkner, J., Ahlrichs, J., Fischer, E., Fuchs, M., Knopf, T., Rösch, M., Scholten, T., Kühn, P.  
1088 2018. Land use dynamics derived from colluvial deposits and bogs in the Black Forest,  
1089 Germany. *Journal of Plant Nutrition Soil Science* 181(2), 240–260,  
1090 <https://doi.org/10.1002/jpln.201700249>.
- 1091 67. Higuera, P.E., Brubaker, L.B., Anderson, P.M., Hu, F.S., Brown, T.A., 2009. Vegetation  
1092 mediated the impacts of postglacial climate change on fire regimes in the south-central  
1093 Brooks Range, Alaska. *Ecological Monographs* 79, 201–219, [https://doi.org/10.1890/07-](https://doi.org/10.1890/07-2019.1)  
1094 [2019.1](https://doi.org/10.1890/07-2019.1).
- 1095 68. Higuera, P.E., Gavin, D.G., Bartlein, P.J., Hallett, D.J., 2010. Peak detection in sediment-  
1096 charcoal records: Impacts of alternative data analysis methods on fire-history interpretations.  
1097 *International Journal of Wildland Fire* 19, 996–1014, <https://doi.org/10.1071/WF09134>.
- 1098 69. Hill, M.O., 1973. Diversity and Evenness: A Unifying Notation and Its Consequences.  
1099 *Ecology* 54, 427–432, <https://doi.org/10.2307/1934352>.
- 1100 70. Hölzl, R. 2010. Historicizing sustainability: German scientific forestry in the eighteenth and  
1101 nineteenth centuries. *Science as Culture* 19(4), 431–  
1102 460, <https://doi.org/10.1080/09505431.2010.519866>
- 1103 71. Houston Durrant, T., de Rigo, D., Caudullo, G., 2016. *Pinus sylvestris* in Europe:  
1104 distribution, habitat, usage and threats. In: San-Miguel-Ayanz, J., de Rigo, D., Caudullo, G.,  
1105 Houston Durrant, T., Mauri, A. (Eds.), *European Atlas of Forest Tree Species*. Publ. Off. EU,  
1106 Luxembourg, pp. e016b94+
- 1107 72. Josefsson, T., Hörnberg, G., Östlund, L., 2009. Long-term human impact and vegetation  
1108 changes in a Boreal Forest Reserve: Implications for the Use of Protected Areas as  
1109 Ecological References. *Ecosystems* 12, 1017–1036, [https://doi.org/10.1007/s10021-009-](https://doi.org/10.1007/s10021-009-9276-y)  
1110 [9276-y](https://doi.org/10.1007/s10021-009-9276-y).
- 1111 73. Kapustka, K., Walls, M., Eigner, J. 2019. Beginnings of mountain settlement in Czech  
1112 Republic - a case study from the Bohemian Forest. In: Pelisiak A, Nowak M and Astaloş C  
1113 (Eds.) *People in the Mountains – Current Approaches to the Archaeology of Mountainous*  
1114 *Landscapes*. Oxford: Archaeopress\_Archaeology, pp. 185–195.

- 1115 74. Karger, D.N., Nobis, M.P., Normand, S., Graham, C.H., Zimmermann, N., 2023. CHELSA-  
1116 TraCE21k – High resolution (1 km) downscaled transient temperature and precipitation data  
1117 since the Last Glacial Maximum. *Climates of the Past* 19, 439–456,  
1118 <https://doi.org/10.5194/cp-19-439-2023>
- 1119 75. Katz, N.J., Katz, S.V., Skobeyeva, E.I. 2007. Atlas of plant remains in peat (in Russian).  
1120 Nedra-press, Moscow.
- 1121 76. Kelly, R.F., Higuera, P.E., Barrett, C.M., Hu, F.S., 2011. A signal-to-noise index to quantify  
1122 the potential for peak detection in sediment-charcoal records. *Quaternary Research* 75, 11–  
1123 17, <https://doi.org/10.1016/j.yqres.2010.07.011>.
- 1124 77. Kolář, J., Dobrovolný, P., Szabó, P., Mikita, T., Kyncl, T., Kyncl, J., Sochová, I., Rybníček,  
1125 M. 2021. Wood species utilization for timber constructions in the Czech lands over the  
1126 period 1400–1900. *Dendrochronologia*, 70, 125900,  
1127 <https://doi.org/10.1016/j.dendro.2021.125900>.
- 1128 78. Kolář, J., Macek, M., Tkáč, P., Novák, Abraham, V., 2022. Long-term demographic trends  
1129 and spatio-temporal distribution of past human activity in Central Europe: Comparison of  
1130 archaeological and palaeoecological proxies. *Quaternary Science Reviews* 297, 107834,  
1131 <https://doi.org/10.1016/j.quascirev.2022.107834>.
- 1132 79. Kothieringer, K., Walser, C., Dietre, B., Reitmaier, T., Haas, J.N., Lambers, K. 2015. High  
1133 impact: early pastoralism and environmental change during the Neolithic and Bronze Age in  
1134 the Silvretta Alps (Switzerland/Austria) as evidenced by archaeological, palaeoecological  
1135 and pedological proxies. *Zeitschrift für Geomorphologie* 59, 177–198,  
1136 [10.1127/zfg\\_suppl/2015/S-59210](https://doi.org/10.1127/zfg_suppl/2015/S-59210).
- 1137 80. Kozáková, R., Bobek, P., Dreslerová, D., Abraham, V., Svobodová-Svitavská, H., 2020. The  
1138 prehistory and early history of the Šumava Mountains (Czech Republic) as seen through  
1139 anthropogenic pollen indicators and charcoal data. *The Holocene* 31(1), 145–159,  
1140 <https://doi.org/10.1177/0959683620961484>.
- 1141 81. Kroll, H. 1988. Das Allerletzte. *Cenococcum geophilum*. – *Archäologische Informationen*.  
1142 *Mitteilungen zur Ur- und Frühgeschichte* 11(1), 111.
- 1143 82. Krzystek, P., Serebryanyk, A., Schnörr, C., Červenka, J., Heurich, M., 2020. Large-scale  
1144 mapping of tree species and dead trees in Šumava National Park and Bavarian Forest  
1145 National Park using lidar and multispectral imagery. *Remote Sensing* 12(4), 661,  
1146 <https://doi.org/10.3390/rs12040661>.
- 1147 83. Lang, G., Ammann, B., Behre, K.-E., Tinner, W., 2023. *Quaternary Vegetation Dynamics of*  
1148 *Europe*. Haupt, Bern.
- 1149 84. Lestienne, M., Jamrichová, E., Kuosmanen, N., Diaconu, A.-C., Schafstall, N., Goliáš, V.,  
1150 Kletetschka, G., Šulc, V., Kuneš, P. 2023. Development of high diversity beech forest in the  
1151 eastern Carpathians. *Journal of Biogeography* 50, 699–714,  
1152 <https://doi.org/10.1111/jbi.14562>.
- 1153 85. Lutz, E., and Pernicka, E., 2013. Prehistoric copper from the Eastern Alps. *Open*  
1154 *Archaeometry*, 1(1), 1–25, <https://doi.org/10.4081/arc.2013.e25>.

- 1155 86. Mateo-Beneito, A., Florescu, G., Tátosová, J., Carter, V.A, Chiverrell, R., Heiri, H., Vasiliev,  
1156 I., Kuosmanen, N., Kuneš, P. 2024. Multi-proxy temperature and environmental  
1157 reconstruction during the Late Glacial and Early Holocene in the Bohemian Forest, Central  
1158 Europe. *Quaternary Science Reviews* 331, 108647,  
1159 <https://doi.org/10.1016/j.quascirev.2024.108647>.
- 1160 87. Matthews, A and Briffa, K.R. 2005. The ‘little ice age’: re-evaluation of an evolving concept.  
1161 *Geografiska Annaler: Series A, Physical Geography* 87(1), 17–36,  
1162 <https://doi.org/10.1111/j.0435-3676.2005.00242.x>.
- 1163 88. Mazei, Y., Tsyganov, A., 2006. *Freshwater Testate Amoebae*. KMK, Moscow.
- 1164 89. Merkt, J., Streif, H.J., 1970. Stechrohrbohrgeräte für limnische und marine  
1165 Lockersedimente. *Geologisches Jahrbuch* 88, 137–148.
- 1166 90. Mustaphi, C.J.C., Pisaric, M.F.J., 2014. A classification for macroscopic charcoal  
1167 morphologies found in Holocene lacustrine sediments. *Progress in Physical Geography* 38,  
1168 734–754, <https://doi.org/10.1177/0309133314548886>.
- 1169 91. Oksanen, J., Blanchet, G.B., Friendly, M., Kindt, R., Legendre, P., McGlinn, D., Minchin,  
1170 P.R., O’Hara, R.B., Simpson, G.L., Solymos, P., Stevens, M.H.H., Szoecs, E., Wagner, H.,  
1171 2017. *vegan: Community Ecology Package*. R package version 2.4-1. [https://CRAN.R-](https://CRAN.R-project.org/package=vegan)  
1172 [project.org/package=vegan](https://CRAN.R-project.org/package=vegan).
- 1173 92. Pigott, C.D. 1982. Survival of mycorrhiza formed by *Cenococcum geophilum* Fr. in dry  
1174 soils. *New Phytologist* 92, 513–517, <http://www.jstor.org/stable/2434235>.
- 1175 93. Pini, R., Ravazzi, C., Raiteri, L., Guerreschi, A., Castellano, L., Comolli, R. 2017. From  
1176 pristine forests to high-altitude pastures: An ecological approach to prehistoric human impact  
1177 on vegetation and landscapes in the western Italian Alps. *Journal of Ecology* 105(6), 1580–  
1178 1597, <https://doi.org/10.1111/1365-2745.12767>.
- 1179 94. Ptáková, M., Pokorný, P., Šída, P., Novák, J., Horáček, I., Juříčková, L., Meduna, P., Bezděk,  
1180 A., Myšková, E., Walls, M., Poschlod, P. 2021. From Mesolithic hunters to Iron Age herders:  
1181 a unique record of woodland use from eastern central Europe (Czech Republic). *Vegetation*  
1182 *History and Archaeobotany* 30, 269–286, <https://doi.org/10.1007/s00334-020-00784-0>.
- 1183 95. Punt, W. 1976-1996. *The northwest European pollen flora 1-7*. Elsevier, Amsterdam.
- 1184 96. R Core Team, 2023. *R: A language and environment for statistical computing*. R Foundation  
1185 for Statistical Computing, Vienna, Austria. <https://www.R-project.org/>
- 1186 97. Reimer, P.J., Austin, W.E.N., Bard, E., Bayliss, A., Blackwell, P.G., Bronk Ramsey, C.,  
1187 Butzin, M., Cheng, H., Edwards, R.L., Friedrich, M., Grootes, P.M., Guilderson, T.P.,  
1188 Hajdas, I., Heaton, T.J., Hogg, A.G., Hughen, K.A., Kromer, B., Manning, S.W., Muscheler,  
1189 R., Palmer, J.G., Pearson, C., Van Der Plicht, J., Reimer, R.W., Richards, D.A., Scott, E.M.,  
1190 Southon, J.R., Turney, C.S.M., Wacker, L., Adolphi, F., Büntgen, U., Capano, M., Fahrni,  
1191 S.M., Fogtmann-Schulz, A., Friedrich, R., Köhler, P., Kudsk, S., Miyake, F., Olsen, J.,  
1192 Reinig, F., Sakamoto, M., Sookdeo, A., Talamo, S., 2020. The IntCal20 Northern  
1193 Hemisphere Radiocarbon Age Calibration Curve (0-55 cal kBP). *Radiocarbon* 62, 725–757.  
1194 <https://doi.org/10.1017/RDC.2020.41>



- 1195 98. Rey, F., Schwörer, C., Gobet, E., Colombaroli, D., van Leeuwen, J.F.N., Schleiss, S., Tinner,  
1196 W., 2013. Climatic and human impacts on mountain vegetation at Lauenensee (Bernese Alps,  
1197 Switzerland) during the last 14,000 years. *The Holocene* 23, 1415–1427,  
1198 <https://doi.org/10.1177/0959683613489585>.
- 1199 99. Rey, F., Gobet, E., Schwörer, C., Wey, O., Hafner, A., Tinner, W. 2019. Causes and  
1200 mechanisms of synchronous succession trajectories in primeval Central European mixed  
1201 *Fagus sylvatica* forests. *Journal of Ecology* 107, 1392–1408, [https://doi.org/10.1111/1365-](https://doi.org/10.1111/1365-2745.13121)  
1202 [2745.13121](https://doi.org/10.1111/1365-2745.13121).
- 1203 100. Robin, V., Bork, H-R., Nadeau, M-J., Nelle, O. 2013. Fire and forest history of central  
1204 European low mountain forest sites based on soil charcoal analysis: The case of the eastern  
1205 Harz. *The Holocene* 24(1), 35–47, <https://doi.org/10.1177/0959683613515727>.
- 1206 101. Rösch, M., 2000. Long-term human impact as registered in an upland pollen profile from  
1207 the southern Black Forest, south-western Germany. *Vegetation History and Archaeobotany*  
1208 9, 205–218, <https://doi.org/10.1007/BF01294635>.
- 1209 102. Schafstall N, Helena Svitavská-Svobodová H, Kadlec M, Gařka M, Kuneř P, Bobek P,  
1210 Goliáš V, Pech P, Nývlt D, Hubený P, Kuosmanen N, Carter VA, Florescu G. 2024. The  
1211 absence of disturbances promoted the expansion of silver fir (*Abies alba*) in the Bohemian  
1212 Forest under drier conditions. *Palaeogeography, Palaeoclimatology, Palaeoecology* 653(1),  
1213 111950, <https://doi.org/10.1016/j.palaeo.2023.111950>.
- 1214 103. Schmidl, A., Kofler, W., Oeggl-Wahlmüller, N., Oeggl, K.D., 2005. Land use in the  
1215 eastern Alps during the Bronze Age - an archaeobotanical case study of a hilltop settlement  
1216 in the Montafon (western Austria). *Archaeometry* 47(2), 455–470,  
1217 <https://doi.org/10.1111/j.1475-4754.2005.00213.x>.
- 1218 104. Schwörer, C., Colombaroli, D., Kaltenrieder, P., Rey, F., Tinner, W., 2015. Early human  
1219 impact (5000-3000 BC) affects mountain forest dynamics in the Alps. *Journal of Ecology*  
1220 103, 281–295, <https://doi.org/10.1111/1365-2745.12354>.
- 1221 105. Schumacher, M., Schier, W., Schütt, B., 2016. Mid-Holocene vegetation development  
1222 and herding-related interferences in the Carpathian region. *Quaternary International* 415,  
1223 253–267, <https://doi.org/10.1016/j.quaint.2015.09.074>.
- 1224 106. Šída, P., Fröhlich, J., Chvojka, O. 2008. Pozdně paleolitická a mezolitická stanoviřte na  
1225 horní Vltavě u Perneku. Nové poznatky o předneolitickém osídlení Lipenska, Archeologické  
1226 výzkumy v jižních Čechách 21, 3–29.
- 1227 107. Šída, P., Eigner, J., Fröhlich, J., Moravcová, M. and Franzeová, D. 2011. Doba kamenná  
1228 v povodí horní Otavy. Plzeň, Západočeská univerzita v Plzni.
- 1229 108. Šída, P., Franzeová, D., Moravcová, M. 2012. Raw material sources and the possibility of  
1230 studying hunter-gatherer mobility as seen on selected Late Upper Palaeolithic and Mesolithic  
1231 Sites in Bohemia. *Natural Sciences in Archaeology* 3(1), 117–129.
- 1232 109. Stockmarr, J. 1972. Tablets with spores used in absolute pollen analysis. *Pollen Spores*  
1233 13, 614–621.

- 1234 110. Šumberová, K., Hájková, P., Chytrý, M., Hroudová, Z., Sádlo, J., Hájek, M., Hrivnák, R.,  
1235 Navrátilová, J., Hanáková, P., Ekrt, L., Ekrťová, E. 2011. Vegetace rákosin a vysokých ostříc  
1236 (Phragmito-Magno-Caricetea). Marsh vegetation. – In: Chytrý M. (ed.), Vegetace České  
1237 republiky. 3. Vodní a mokřadní vegetace [Vegetation of the Czech Republic 3. Aquatic and  
1238 wetland vegetation], p. 386–579, Academia, Praha.
- 1239 111. Svobodová, H., Soukupová, L., and Reille, M., 2002. Diversified development of  
1240 mountain mires, Bohemian Forest, Central Europe, in the last 13,000 years. Quaternary  
1241 International 91(1), 123–135, [https://doi.org/10.1016/S1040-6182\(01\)00106-9](https://doi.org/10.1016/S1040-6182(01)00106-9).
- 1242 112. Svobodová, H., Reille, M., and Goeury, C., 2001. Past vegetation dynamics of Vltavský  
1243 luh, upper Vltava River valley in the Šumava mountains, Czech Republic. Vegetation  
1244 History and Archaeobotany 10(4), 185–199, <https://doi.org/10.1007/PL00006930>.
- 1245 113. Tinner, W., Conedera, M., Ammann, B., Gaggeler, H.W., Gedye, S., Jones, R., Sagesser,  
1246 B. 1998. Pollen and charcoal in lake sediments compared with historically documented forest  
1247 fires in southern Switzerland since AD 1920. The Holocene 8, 31–42,  
1248 <https://doi.org/10.1191/095968398667205430>.
- 1249 114. Tinner, W., Lang, G., Schwörer, C. 2023. Treeline and timberline dynamics. In: Lang, G.,  
1250 Ammann, B., Behre, K.-E., Tinner, W., 2023. Quaternary Vegetation Dynamics of Europe.  
1251 Haupt, Bern, pp. 455–466.
- 1252 115. Tinner, W. 2023. Long-term disturbance ecology. In: Lang, G., Ammann, B., Behre, K.-  
1253 E., Tinner, W., 2023. Quaternary Vegetation Dynamics of Europe. Haupt, Bern, pp. 467–  
1254 485.
- 1255 116. Tomlinson, P. 1985. An aid to the identification of fossil buds, bud-scales and catkin-  
1256 bracts of British trees and shrubs. Circaea 3, 45–130.
- 1257 117. Turetsky, M.R., Benscoter, B., Page, S., Rein, G., van der Werf, G.R., Watts, A. 2014.  
1258 Global vulnerability of peatlands to fire and carbon loss. Nature Geoscience 8, 11–14,  
1259 <https://doi.org/10.1038/ngeo2325>.
- 1260 118. Umbanhowar, C.E., Mcgrath, M.J., 1998. Experimental production and analysis of  
1261 microscopic charcoal from wood, leaves and grasses. The Holocene, 8(3), 341–346,  
1262 <https://doi.org/10.1191/095968398666496051>.
- 1263 119. van Geel, G., 1978. A paleoecological study of Holocene peat bog sections in Germany  
1264 and the Netherlands, based on the analysis of pollen, spores, and macro- and microscopic  
1265 remains of fungi, algae, cormophytes and animals. Review of Palaeobotany and Palynology  
1266 25(1), 1–120, 10.1016/0034-6667(78)90040-4.
- 1267 120. Vannièrè, B., Blarquez, O., Rius, D., Doyen, E., Brücher, T., Colombaroli, D., Connor,  
1268 S., Feurdean, A., Hickler, T., Kaltenrieder, P., Lemmen, C., Leys, B., Massa, C., Olofsson, J.  
1269 2016. 7000-year human legacy of elevation-dependent European fire regimes. Quaternary  
1270 Science Reviews, 132, 206–212, <https://doi.org/10.1016/j.quascirev.2015.11.012>.
- 1271 121. Vencl, S. 2006. Nejstarší osídlení jižních Čech. Praha, Archeologický ústav Akademie  
1272 věd ČR.

- 1273 122. Vera, F.W.M., 2000. Grazing ecology and forest history. CABI Publishing, Wallingford.  
1274 pp 1–506.
- 1275 123. Veron, A., Novak, M., Brizova, E., Stepanova, M. 2014. Environmental imprints of  
1276 climate changes and anthropogenic activities in the Ore Mountains of Bohemia (Central  
1277 Europe) since 13 cal. ka BP. *The Holocene* 24(8), 919–931,  
1278 <https://doi.org/10.1177/0959683614534746>.
- 1279 124. Veselý, J., Almquist-Jacobson, H., Miller, L.M., Norton, S.A., Appleby, P., Dixit, A.S.,  
1280 Smol, J.P. 1993. The history and impact of air pollution at Čertovo Lake, southwestern  
1281 Czech Republic. *Journal of Paleolimnology* 8, 211–231,  
1282 <https://doi.org/10.1007/BF00177857>.
- 1283 125. Willis, K.J., and Birks, H.J.B. 2006. What is natural? The need for a long-term  
1284 perspective in biodiversity conservation. *Science* 314, 1261–1265, DOI:  
1285 [10.1126/science.1122667](https://doi.org/10.1126/science.1122667)
- 1286 126. Wood, S.N., 2006. *Generalized Additive Models: an introduction with R*. Boca Raton:  
1287 CRC/Chapman & Hall
- 1288 127. Zlámalová Cílová, Z., Gelnar, M., Randáková, S. 2021. Trends in Colouring Blue Glass  
1289 in Central Europe in Relation to Changes in Chemical Composition of Glass from the Middle  
1290 Ages to Modern Ages. *Mineral* 11(9), 1001, <https://doi.org/10.3390/min11091001>.  
1291

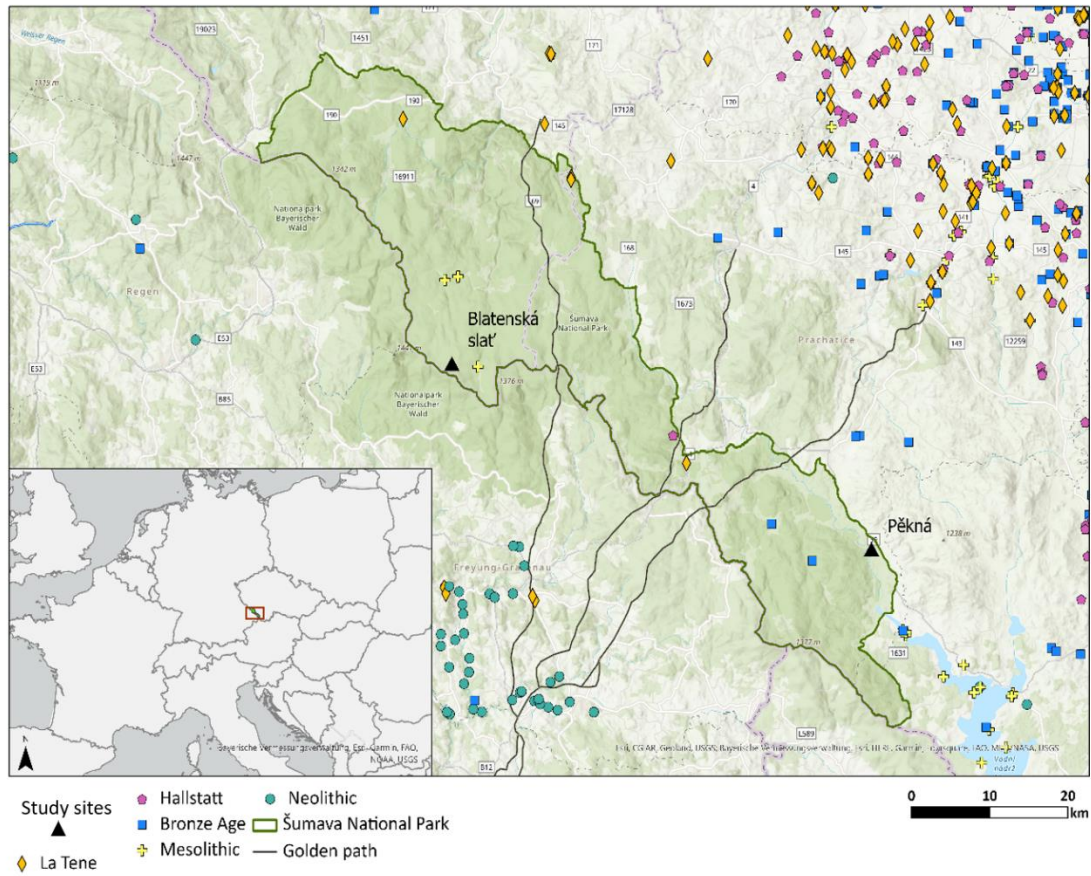


Figure 1. Map showing the location of Pěkná (730 m asl) and Blatenská slat' (1275 m asl) peat bogs located in Šumava National Park on the border of Czechia, Germany and Austria (small inset figure), in relation to known archeological sites (main figure); Mesolithic sites (yellow '+'), Neolithic sites (green dots), Bronze Age sites (blue squares), Early Iron Age – Hallstatt sites (pink hexagon), Late Iron Age – La Tène sites (orange triangles); black triangles are our study sites. The three black lines that transect the Bohemian Forest Ecosystem are known historic trading routes. Image by Č. Čišecký.

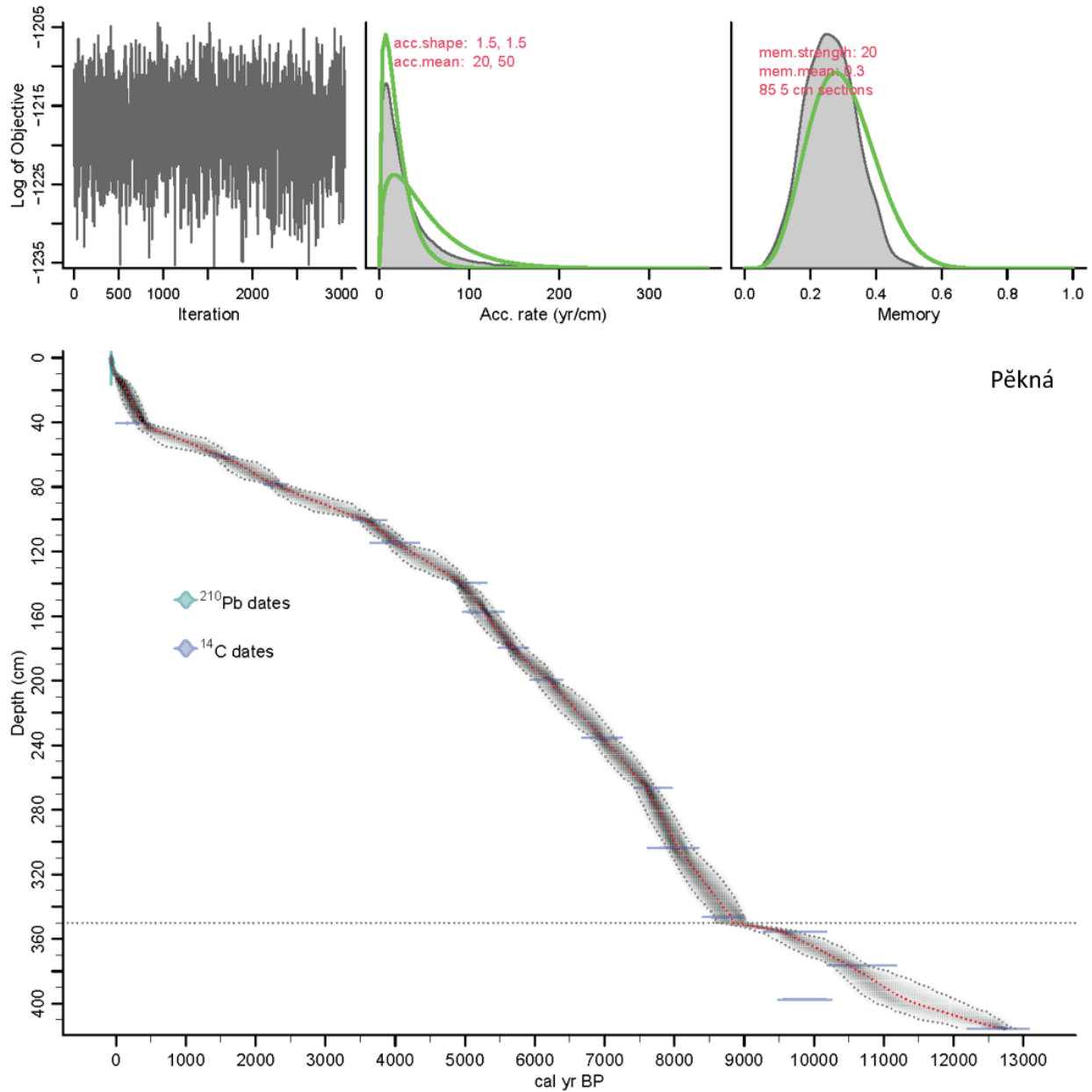


Figure 2. Age-depth model and lithology for Pěkná, Czechia. Age-depth relationships were established using thirteen  $^{14}\text{C}$  dates of bulk peat and macrofossil origin, and a  $^{210}\text{Pb}$  series (Appleby, 1978), and were modeled in ‘rbacon’ (Blaauw and Christen, 2011) using the IntCal20 dataset for  $^{14}\text{C}$  ages (Reimer et al., 2020). The horizontal dotted line represents the sedimentation boundary between decomposed herbaceous peat and *Eriophorum* peat (see lithology in SI Figure 2). Different prior accumulation rate means were used for these two sections.

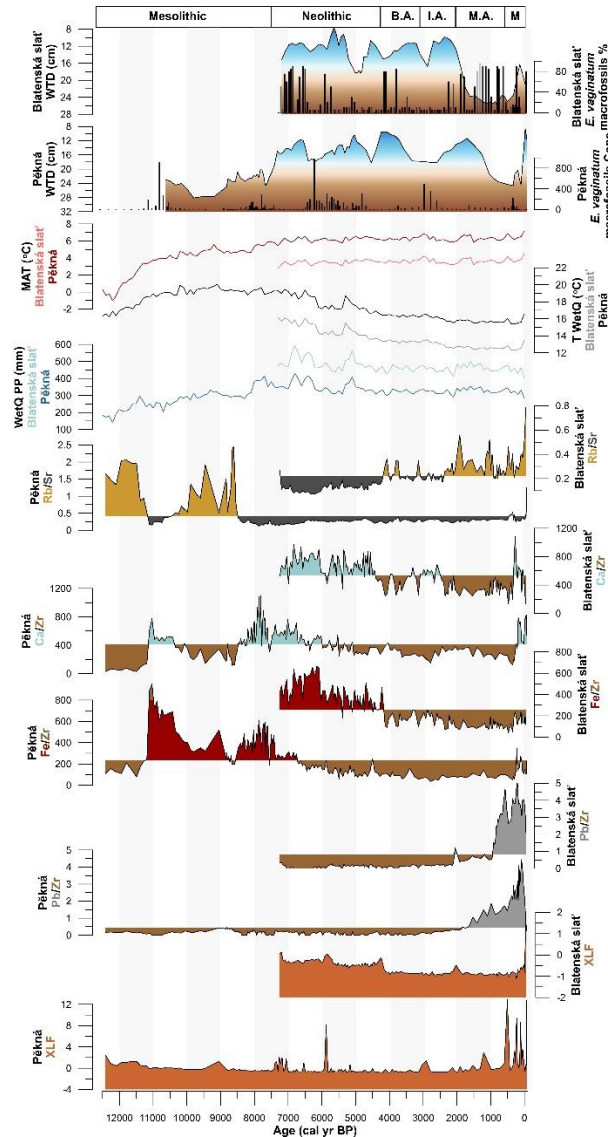


Figure 3. Reconstructed hydroclimate and geochemistry for Pěkná and Blatenská slat'. From top to bottom (with Blatenská slat' presented first since it is higher in elevation (1275 m asl) and Pěkná presented second (mid-elevation site, 730 m asl); Different archaeological time periods; testate amoebae reconstructed water table depths (WTDs; brown = drier, blue = wetter) with *Eriophorum vaginatum* macrofossils, an indicator of dry conditions, overlaid (black vertical bars); CHELSA modeled climate variables including mean annual temperatures (MAT; salmon = Blatenská slat, red = Pěkná), temperature of the wettest quarter (T WetQ; black = Blatenská slat, gray = Pěkná), precipitation for the wettest quarter (WetQ pp; light blue = Blatenská slat, dark blue = Pěkná) (Karger et al., 2023); Rb/Sr, an indicator of mineralogic input (gold = increased mineralogic input, black = decreased mineralogic input); Ca/Zr, an indicator of authigenic Ca (brown = decreased Ca, blue = increased Ca); Fe/Zr, an indicator of authigenic Fe (brown = decreased Fe, red = increased Fe); Pb/Zr, an anthropogenic indicator for mining activity (brown = decreased Pb, gray = increased Pb); low frequency magnetic susceptibility ( $\chi_{LF}$ ), an indicator of erosion (brown curves).

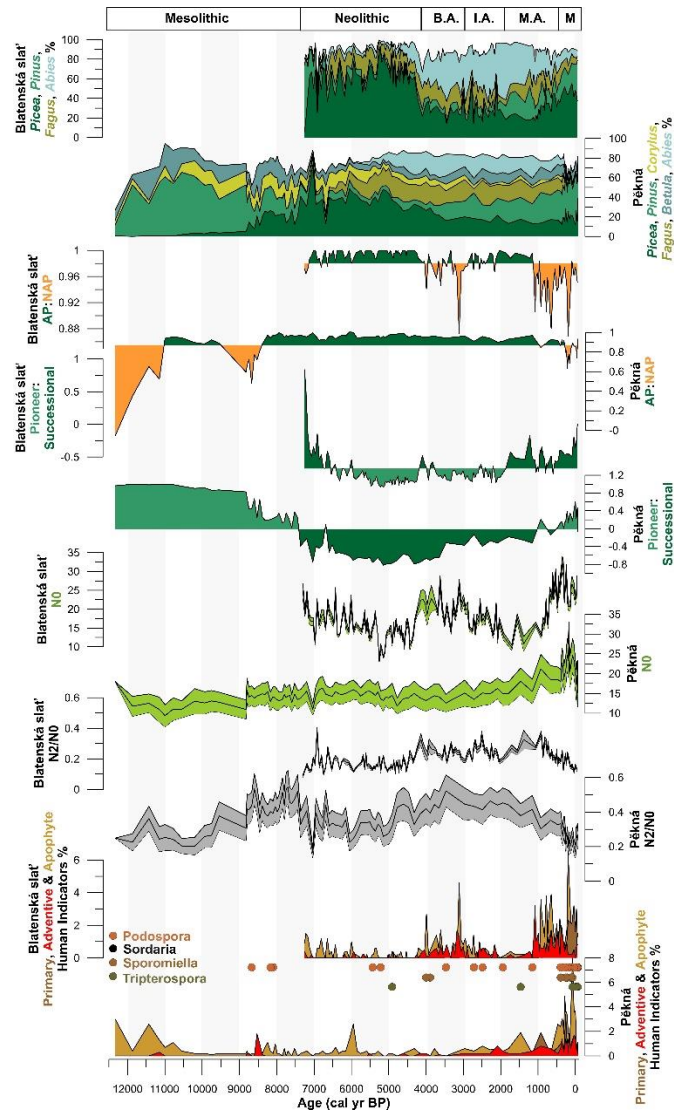


Figure 4. Reconstructed vegetation history for Pěkná and Blatenská slat'. From top to bottom (with Blatenská slat' presented first since it is higher in elevation (1275 m asl) and Pěkná presented second (mid-elevation site, 730 m asl); Different archaeological time periods; Dominant forest canopy pollen percentages (dark green curve = *Picea abies*, light green curve = *Pinus*, yellow curve = *Corylus*, olive curve = *Fagus*, dark blue curve = *Betula*, light blue curve = *Abies*); index of forest openness (arboreal pollen = dark green curve, non-arboreal pollen = orange curve), index of forest succession (light green curve = pioneer tree taxa, dark green curve = successional tree taxa); rarefied pollen richness (N0; green curve with gray confidence intervals) indicating periods of increased pollen diversity; pollen evenness (N2/N0; gray lines) indicating the potential dominance of pollen taxa within an ecosystem; primary (brow curve), adventive (red curve) and apophyte (gold curve) pollen indicator taxa indicating human activities overlaid with coprophilous fungi, an indicator of grazers (*Podospora* = orange dots, *Sordaria* = black dots, *Sporomiella* = brown dots, *Tripterospora* = green dots).

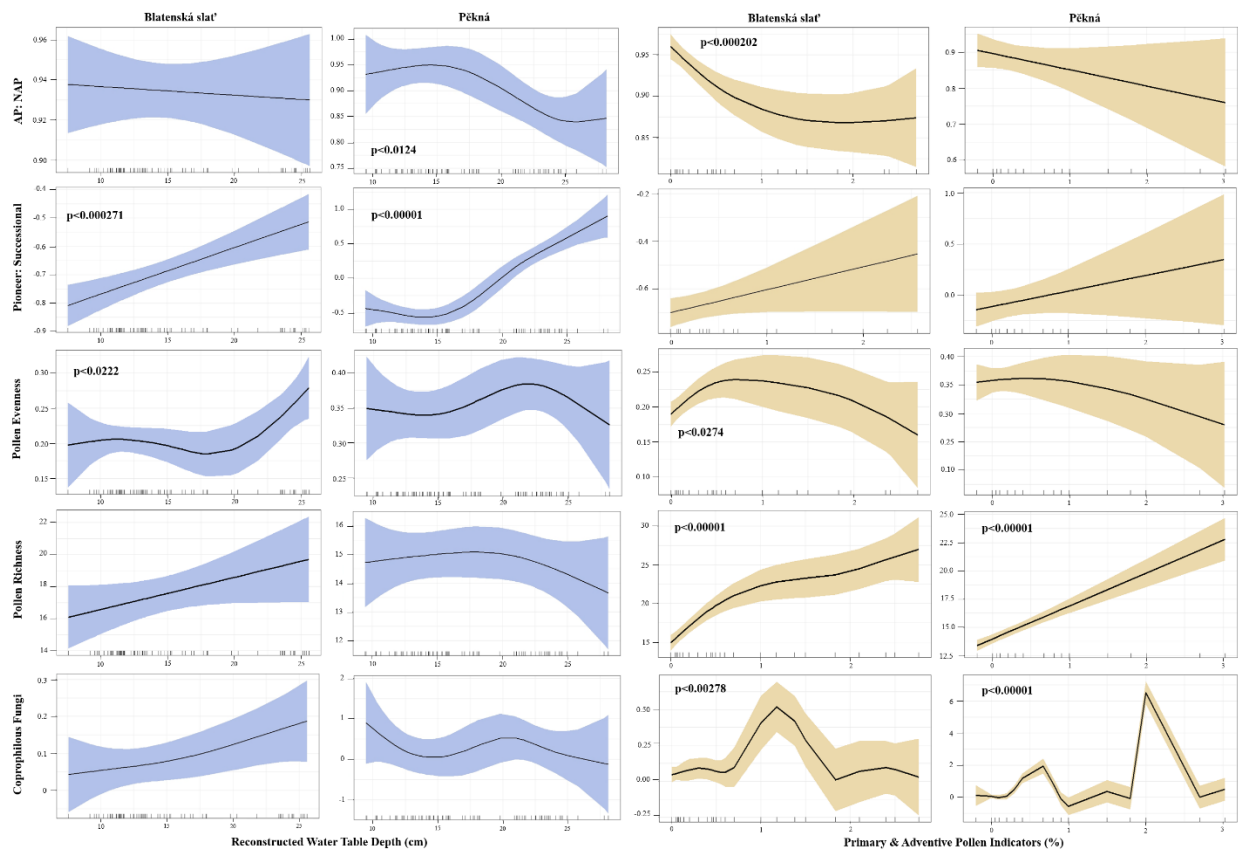


Figure 5. Model response curves showing the relationship between hydroclimate and anthropogenic indicators as independent variables and various forest succession, forest composition and pollen diversity variables at Blatenská slat' and Pěkná, Czechia. Blue curves are results for testate amoebae reconstructed water table depths (WTDs). Yellow curves are results for the sum of primary and adventive pollen indicators following Deza-Aruajo et al. 2020. Bold p-values indicate the relationship is statistically significant.



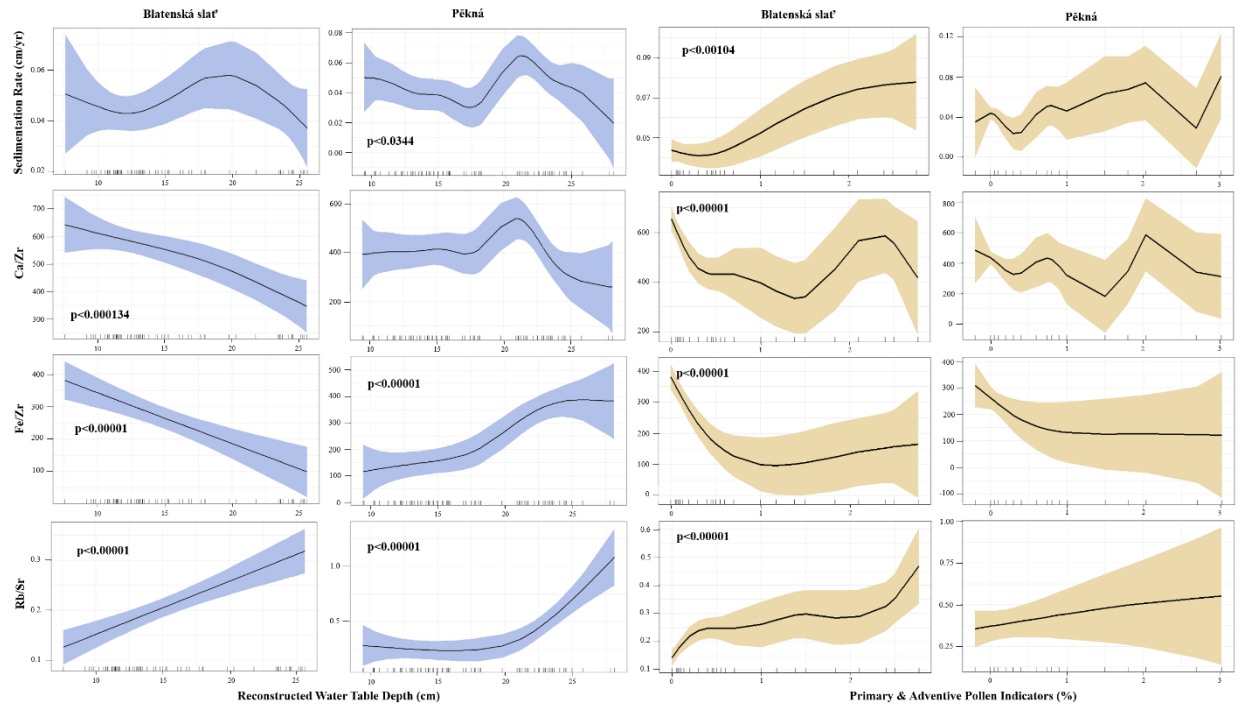


Figure 6. Model response curves showing the relationship between hydroclimate and primary and adventive pollen indicators, (i.e., anthropogenic indicators) as independent variables and various geochemistry variables used as indicators of erosional and depositional activity at Blatenská slat' and Pěkná, Czechia. Blue curves are results for testate amoebae reconstructed water table depths (WTDs). Yellow curves are results for the sum of all primary and secondary pollen indicators. Bold p-values indicate the relationship is statistically significant.

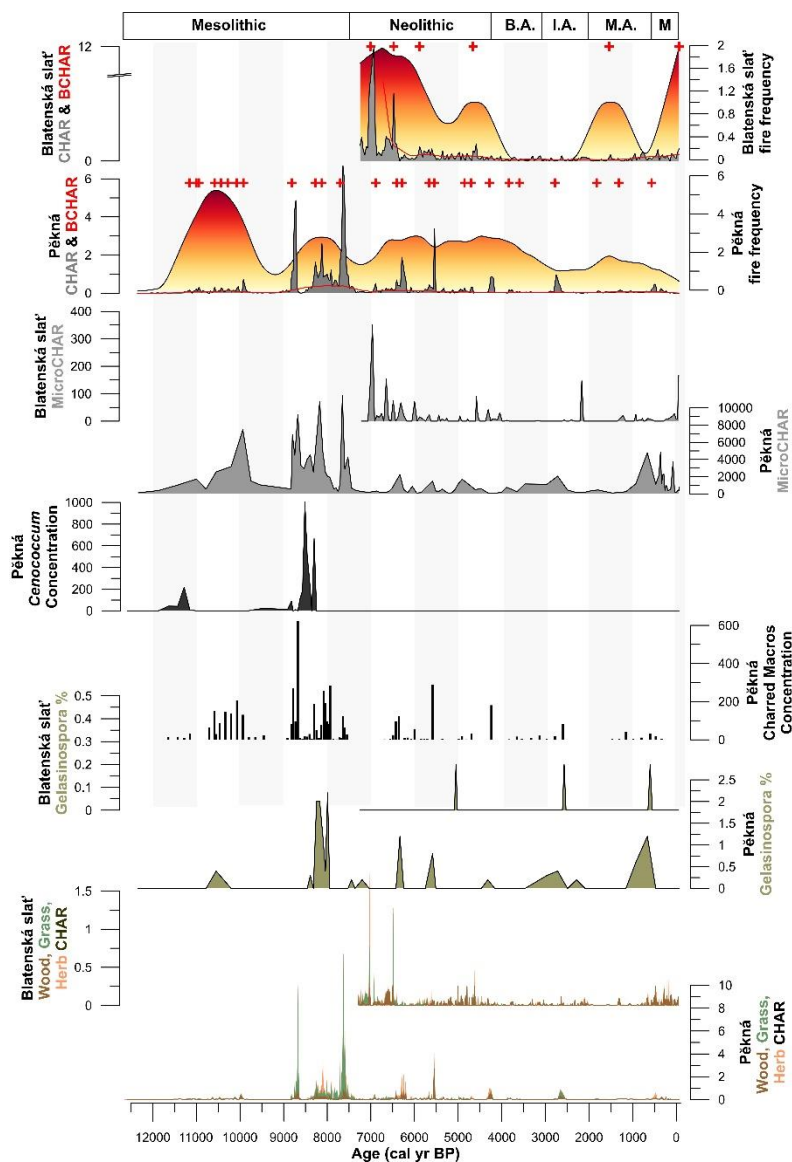


Figure 7. Reconstructed fire history for Pěkná and Blatenská slat'. From top to bottom (with Blatenská slat' presented first since it is higher in elevation (1275 m asl) than Pěkná (730 m asl); Different archaeological time periods; CHAR (particles per  $\text{cm}^{-2} \text{yr}^{-1}$ ) (dark gray curve), with BCHAR (red line) indicates regional fire activity; fire frequency indicates fires/1000 years (filled colour curve); fire episodes are represented with a red '+' symbol; Microcharcoal (particles per  $\text{cm}^{-2} \text{yr}^{-1}$ ) (dark gray curve), indicates regional biomass burning; *Cenococcum geophilum* concentrations (black curve), an indicator of soil erosion after fire (only observed at Pěkná); Charred macrofossil concentrations (black histogram) is the sum of all charred macrofossil data (only observed at Pěkná); *Gelasinospora* percentages (olive curve) indicates fire activity; Wood CHAR (brown curve), Grass CHAR (green curve), and Herb CHAR (salmon curve) indicate fuel source type; presented on a log scale to visually demonstrate the large abundance of woody charcoal.

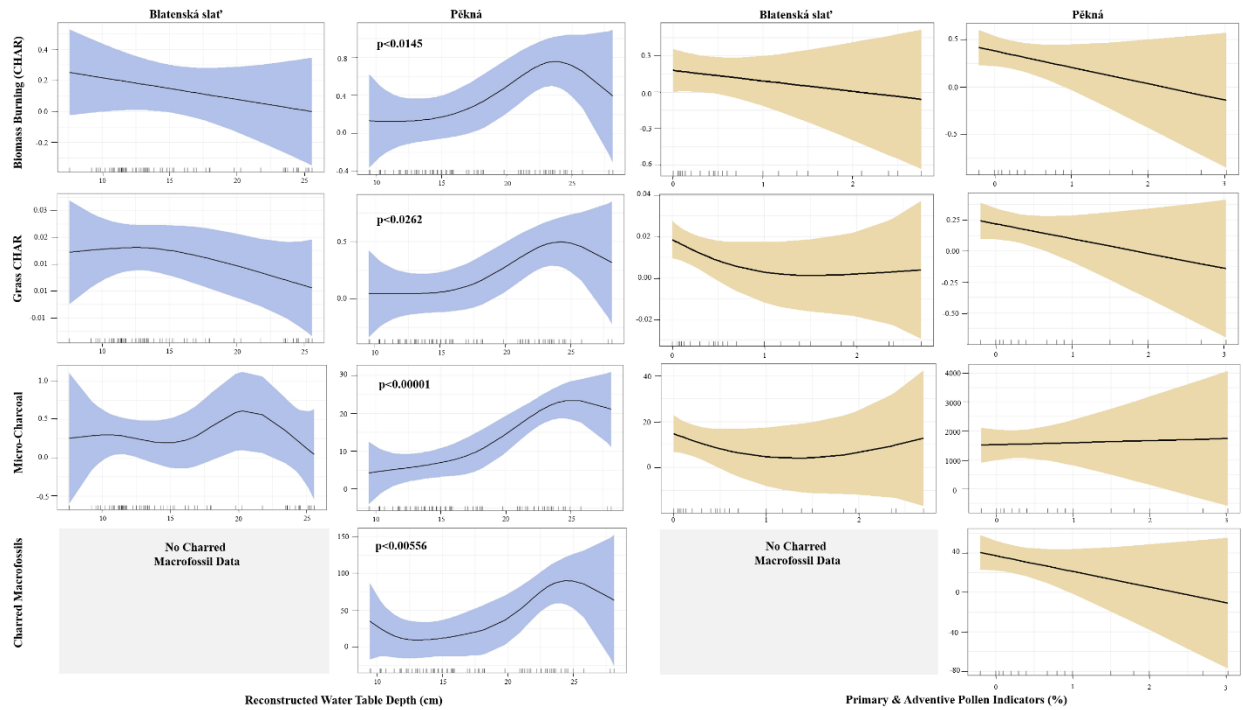


Figure 8. Model response curves showing the relationship between hydroclimate and anthropogenic indicators as independent variables and various fire variables indicator of fire activity at Blatenská slat' and Pěkná, Czechia. Blue curves are results for testate amoebae reconstructed water table depths (WTDs). Yellow curves are results for the sum of primary and adventive pollen indicators following Dezu-Aruajo et al., 2020. Bold p-values indicate the relationship is statistically significant.

Table 1. Age-depth relations for Pěkná, Czechia.

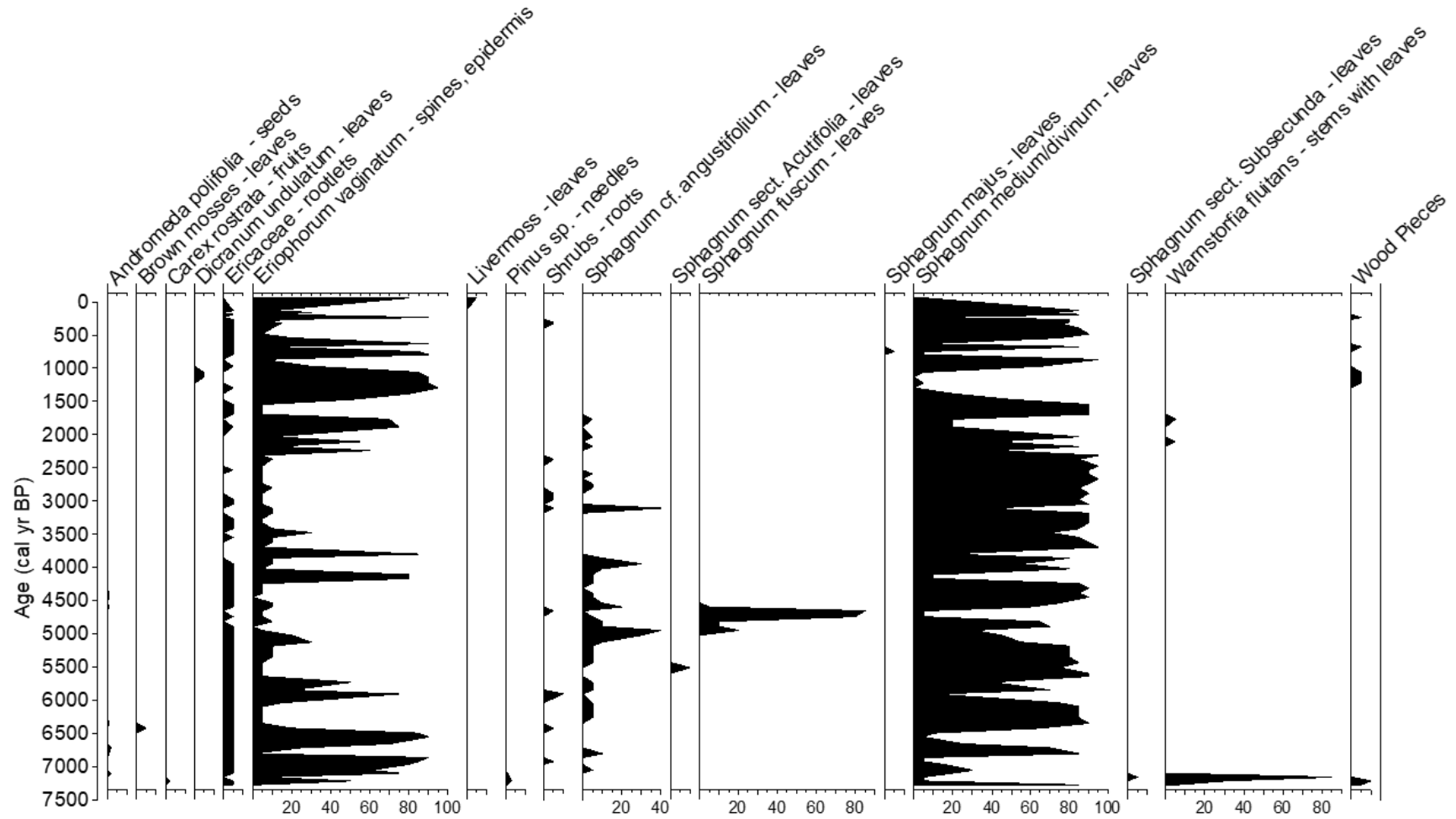
Isotope	Lab Code	Depth (cm)	Age ( $^{210}\text{Pb}$ / $^{14}\text{C}$ yr BP)	Sample Material
$^{210}\text{Pb}$		1	2017 ± 8.4	Bulk peat
$^{210}\text{Pb}$		2	2015 ± 8.3	Bulk peat
$^{210}\text{Pb}$		3	2012 ± 8.3	Bulk peat
$^{210}\text{Pb}$		4	2009 ± 8.4	Bulk peat
$^{210}\text{Pb}$		6	2001 ± 8.5	Bulk peat
$^{210}\text{Pb}$		8	1990 ± 8.8	Bulk peat
$^{210}\text{Pb}$		10	1965 ± 11.4	Bulk peat
$^{210}\text{Pb}$		12	1918 ± 17.3	Bulk peat
$^{14}\text{C}$	DeA-22180	41	250 ± 25	Conifer needle, Ericaceae bud
$^{14}\text{C}$	DeA-26077	62	1653 ± 27	<i>Sphagnum</i> stems
$^{14}\text{C}$	DeA-22181	79	2289 ± 26	<i>Betula</i> twig
$^{14}\text{C}$	DeA-26078	101	3383 ± 38	<i>Sphagnum</i> stems
$^{14}\text{C}$	DeA-23068	115	3649 ± 46	<i>Oxycoccus</i> leaves, pine needle, <i>Carex</i> seeds
$^{14}\text{C}$	DeA-26079	140	4409 ± 36	<i>Sphagnum</i> stems
$^{14}\text{C}$	DeA-22181	158	4576 ± 35	<i>Sphagnum</i> stems
$^{14}\text{C}$	DeA-26080	180	4941 ± 37	<i>Sphagnum</i> stems
$^{14}\text{C}$	DeA-26081	200	5402 ± 41	<i>Sphagnum</i> stems
$^{14}\text{C}$	DeA-22183	236	6101 ± 41	<i>Sphagnum</i> stems
$^{14}\text{C}$	DeA-22184	267	6825 ± 68	Charred <i>Oxycoccus</i> leaves
$^{14}\text{C}$	DeA-22185	304	7143 ± 72	<i>Sphagnum</i> stems
$^{14}\text{C}$	DeA-26082	347	7852 ± 48	<i>Carex</i> seeds
$^{14}\text{C}$	DeA-22186	356	8608 ± 68	<i>Carex</i> seeds
$^{14}\text{C}$	DeA-22187	377	9348 ± 73	<i>Carex</i> seeds
$^{14}\text{C}$	DeA-26083	398	8800 ± 69	<i>Carex</i> seeds and leaf fragments
$^{14}\text{C}$	DeA-22188	416	10746 ± 73	<i>Carex</i> seeds and leaves

Table 2. Pollen taxa used to calculate primary and secondary pollen indicators, indicative of human influence on at the landscape at Pěkná and Blatenská slat', Czechia. Taxa were selected following Dezu-Aruajo et al., 2020.

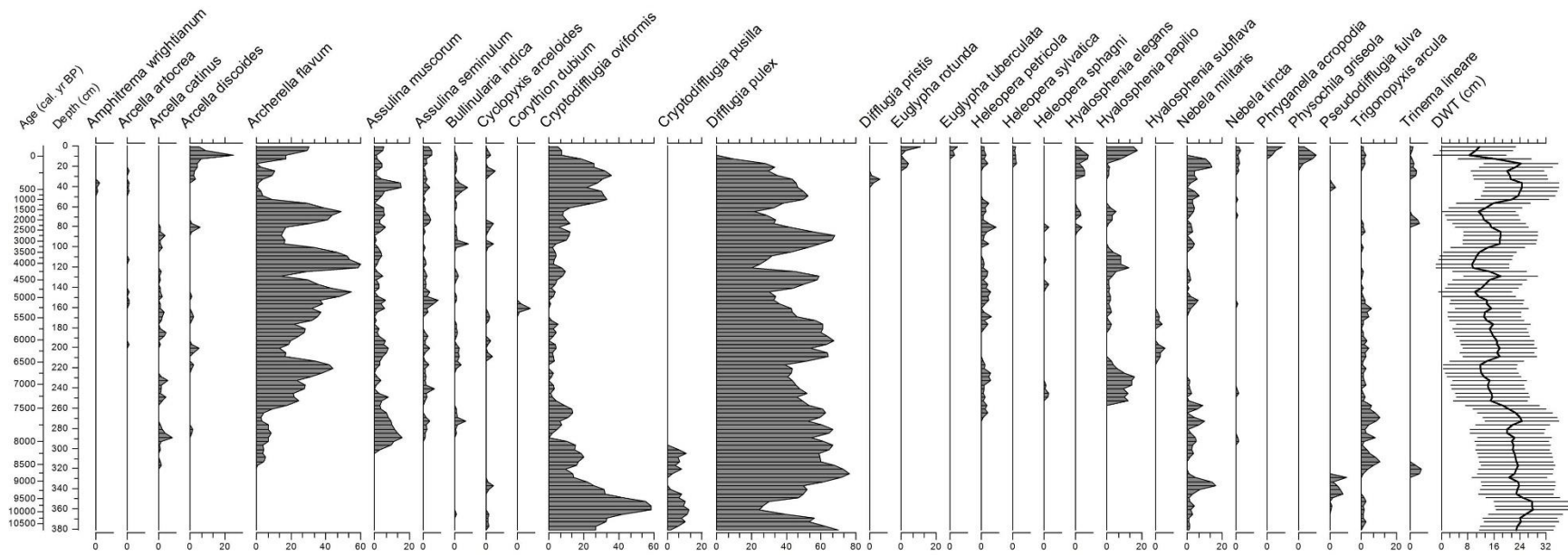
	<b>Pěkná</b>	<b>Blatenská slat'</b>
Primary Indicators	<i>Secale, Juglans</i>	<i>Cannabis-type, Fagopyrum, Juglans, Secale, Triticum-type, Vicia</i>
Secondary Indicators (Adventives)	<i>Plantago lanceolata, Plantago major, Plantago sp., Polygonum aviculare-type</i>	<i>Plantago lanceolata, Plantago major, Plantago sp., Polygonum aviculare-type,</i>
Secondary Indicators (Apophytes)	<i>Juniperus, Calluna vulgaris, Artemisia, Melampyrum, Rumex, Trifolium, Urtica</i>	<i>Artemisia, Calluna vulgaris, Campanula, Juniperus, Melampyrum, Pteridium aquilinum, Rumex, Urtica</i>



SI Figure 1. Full plant macrofossil diagram with core lithology for Pěkná, Czechia. Top panel are tree, shrub and herb macrofossils. Bottom panel are charred macrofossils only.

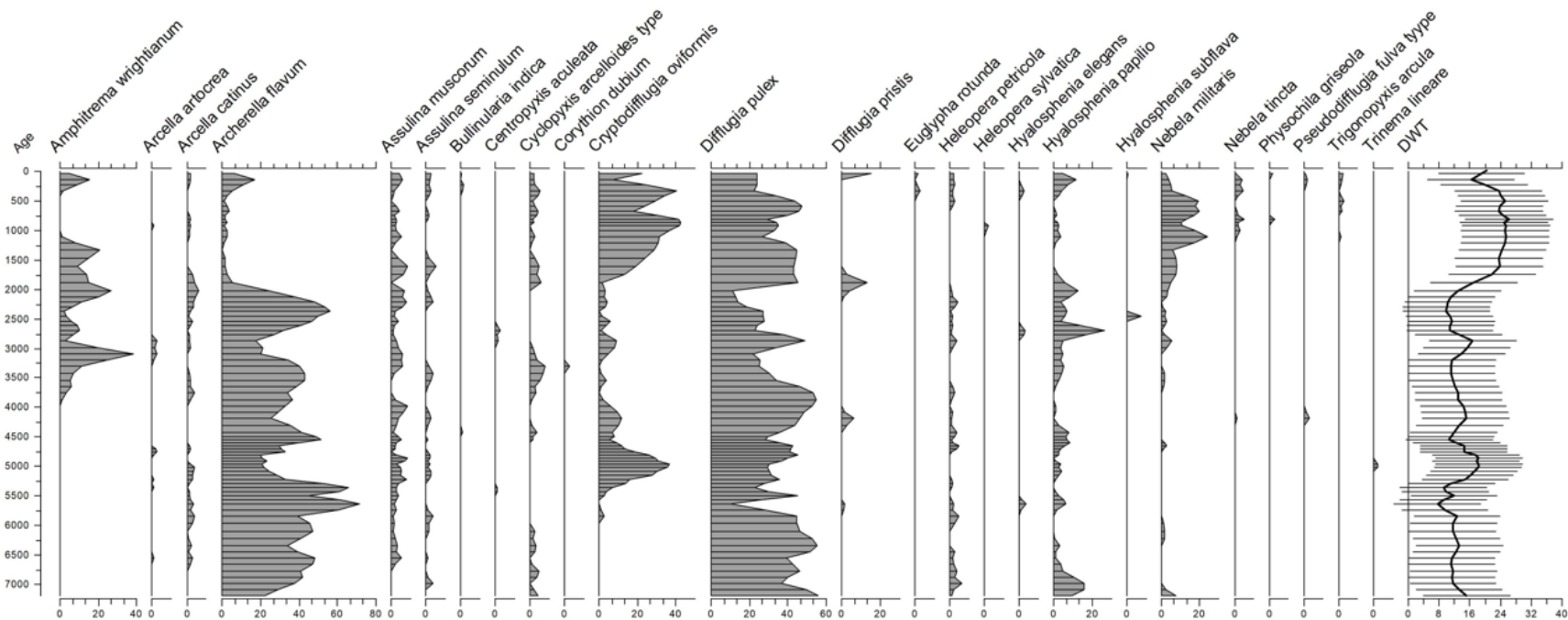


SI Figure 2. Full plant macrofossil diagram for Blatenská slat', Czechia.



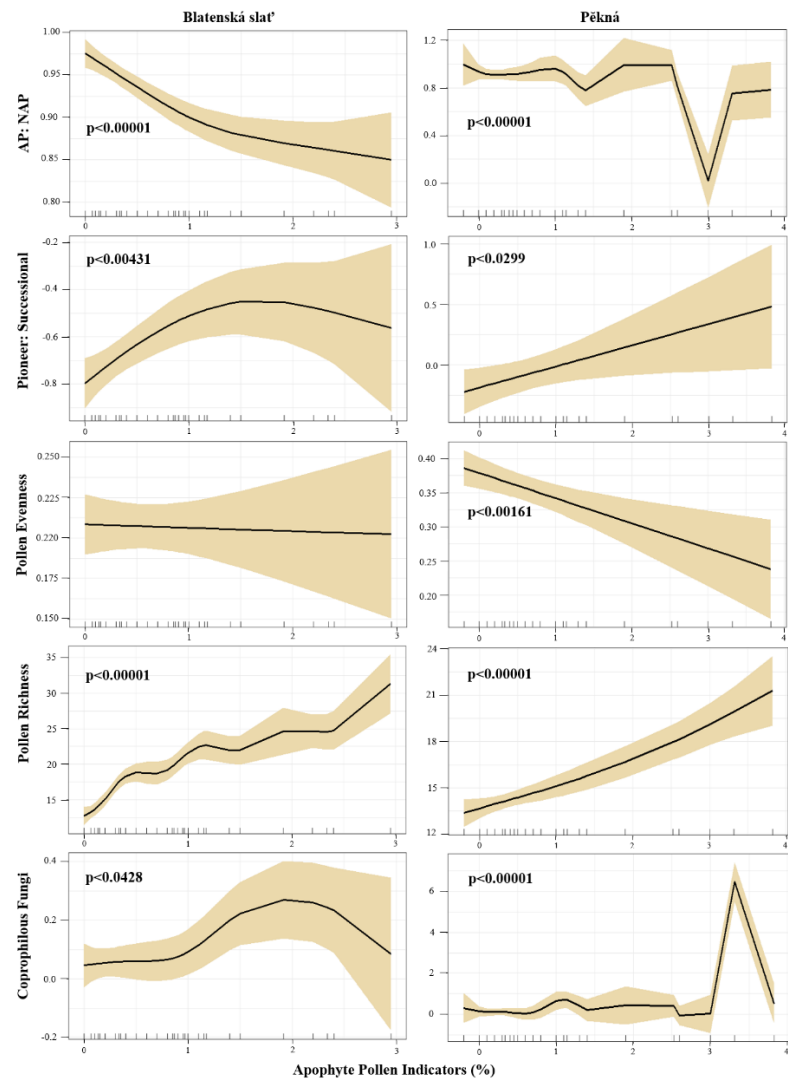
SI Figure 3. Full testate amoebae and reconstructed water table depth diagram for Pěkná, Czechia.



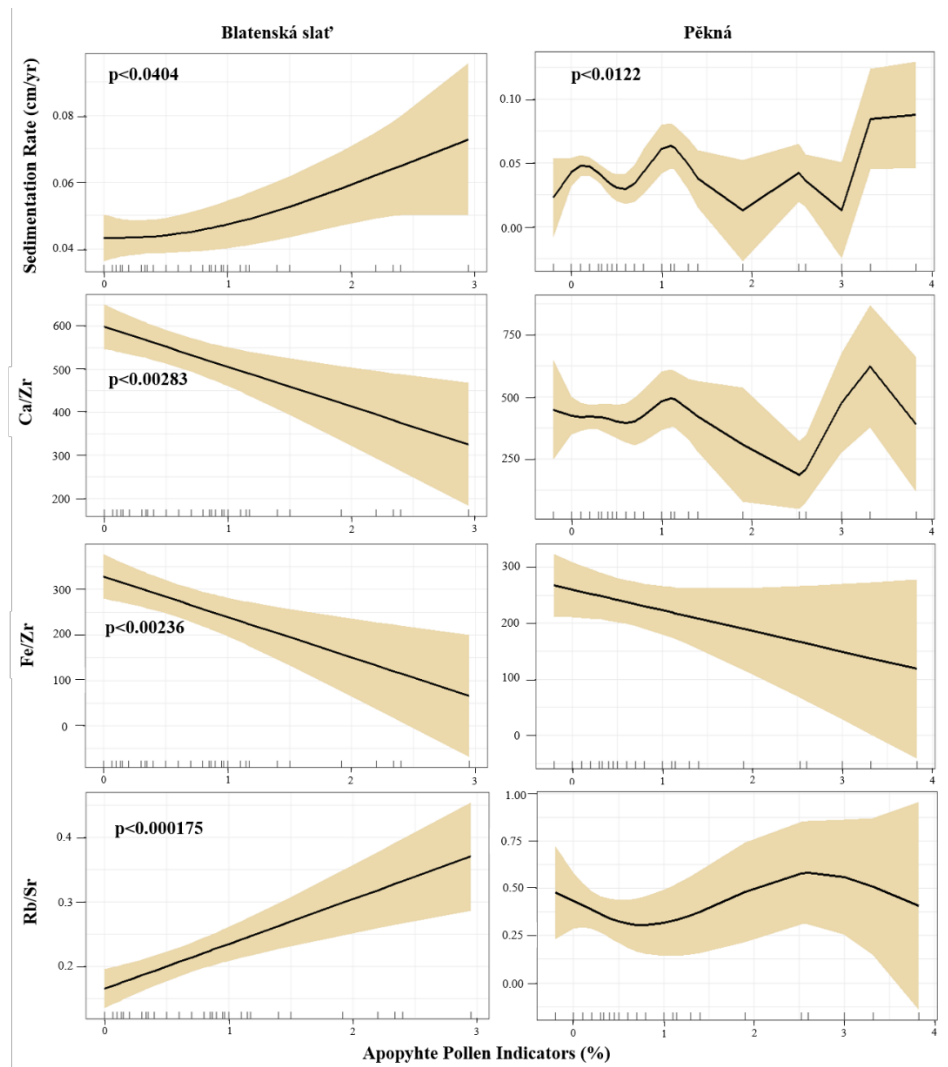


SI Figure 4. Full testate amoebae and reconstructed water table depth diagram for Blatenská slat', Czechia.

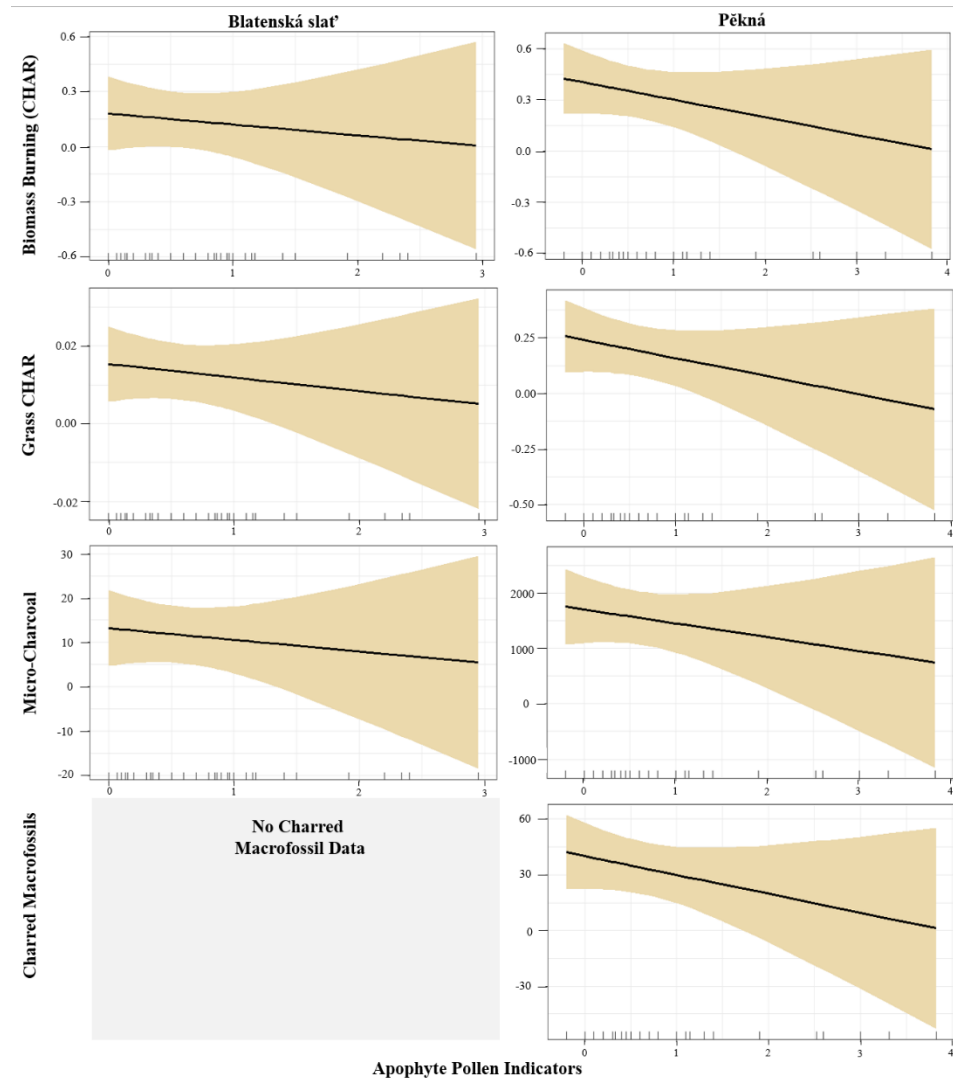




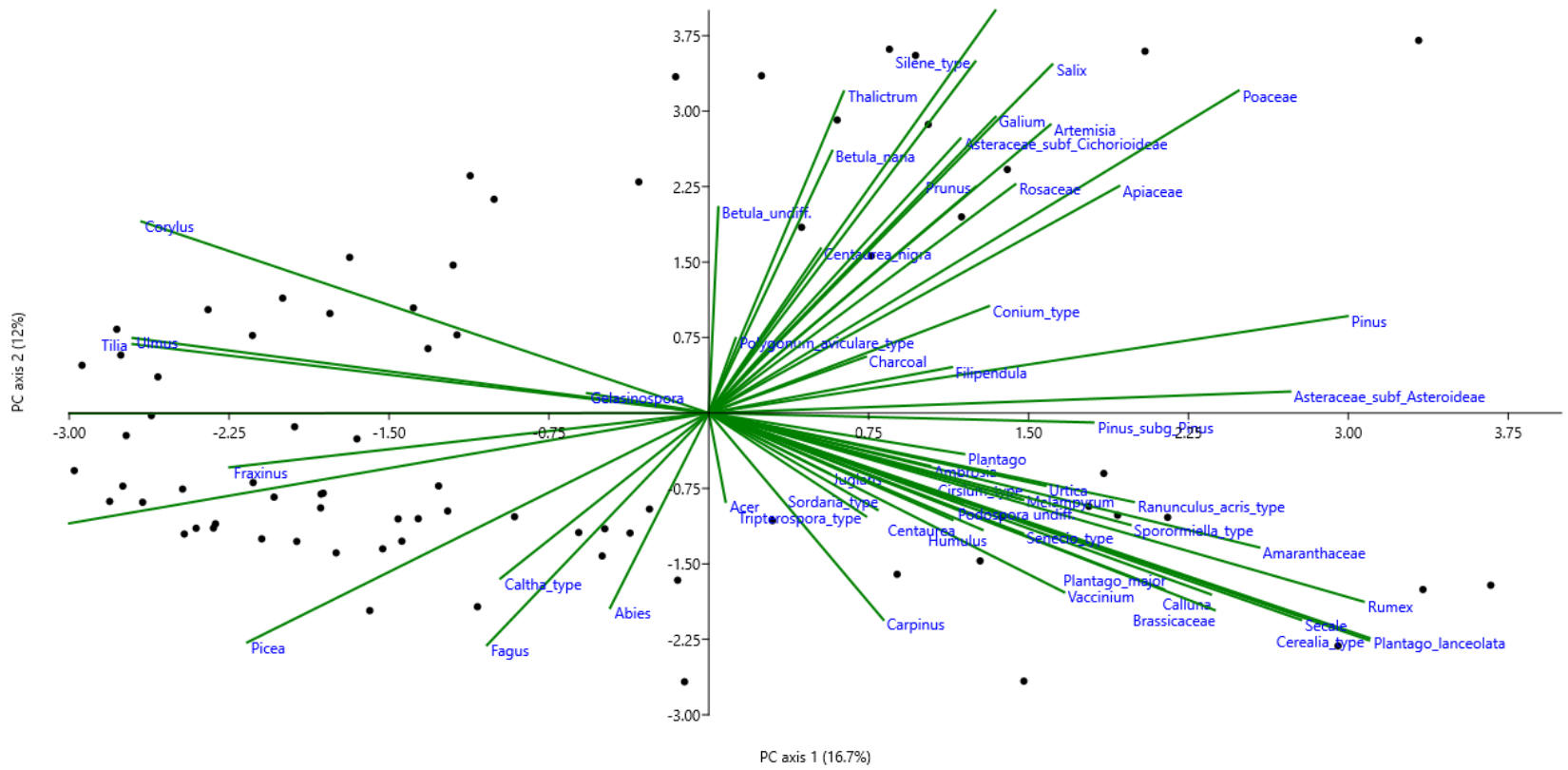
SI Figure 6. Model response curves showing the relationship between apophyte pollen indicators as independent variables and various forest succession, forest composition and pollen diversity variables at Blatenská slat' and Pěkná, Czechia. Bold p-values indicate the relationship is statistically significant.



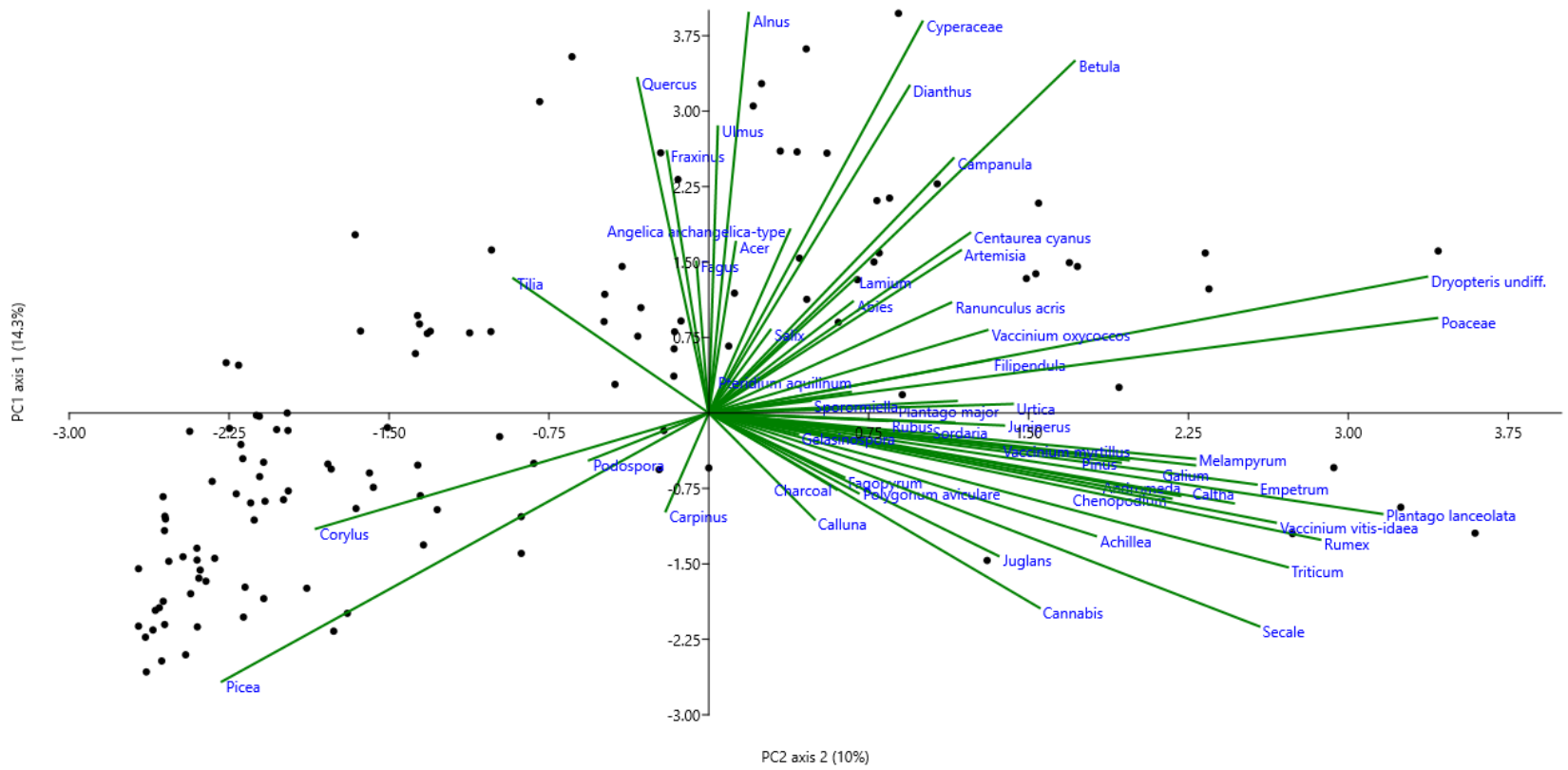
SI Figure 7. Model response curves showing the relationship between apophyte pollen indicators as independent variables and various geochemistry variables used as indicators of erosional and depositional activity at Blatenská slat' and Pěkná, Czechia. Bold p-values indicate the relationship is statistically significant.



SI Figure 8. Model response curves showing the relationship between apophyte pollen as independent variables and various fire variables indicator of fire activity at Blatenská slat' and Pěkná, Czechia. Bold p-values indicate the relationship is statistically significant.



SI Figure 9. PCA results for fossil pollen data from Pěkná, Czechia.



SI Figure 10. PCA results for fossil pollen data from Blatenská slat, Czechia.